

**DOT/FAA/AR-05/14**

Office of Aviation Research  
Washington, D.C. 20591

# **Polymer Flammability**

May 2005

Final Report

This document is available to the U.S. public through the National Technical Information Service (NTIS), Springfield, Virginia 22161.



U.S. Department of Transportation  
**Federal Aviation Administration**

## **NOTICE**

This document is disseminated under the sponsorship of the U.S. Department of Transportation in the interest of information exchange. The United States Government assumes no liability for the contents or use thereof. The United States Government does not endorse products or manufacturers. Trade or manufacturer's names appear herein solely because they are considered essential to the objective of this report. This document does not constitute FAA certification policy. Consult your local FAA aircraft certification office as to its use.

This report is available at the Federal Aviation Administration William J. Hughes Technical Center's Full-Text Technical Reports page: [actlibrary.tc.faa.gov](http://actlibrary.tc.faa.gov) in Adobe Acrobat portable document format (PDF).

**Technical Report Documentation Page**

1. Report No. <b>DOT/FAA/AR-05/14</b>		2. Government Accession No.		3. Recipient's Catalog No.	
4. Title and Subtitle <b>POLYMER FLAMMABILITY</b>				5. Report Date <b>May 2005</b>	
				6. Performing Organization Code	
7. Author(s) <b>Richard E. Lyon and Marc L. Janssens*</b>				8. Performing Organization Report No.	
9. Performing Organization Name and Address <b>*Southwest Research Institute 6220 Culebra Rd. P.O. Drawer 28510 San Antonio, TX 78228-0510</b>				10. Work Unit No. (TRAIS)	
				11. Contract or Grant No.	
12. Sponsoring Agency Name and Address <b>U.S. Department of Transportation Federal Aviation Administration Office of Aviation Research Washington, DC 20591</b>				13. Type of Report and Period Covered <b>Final Report</b>	
				14. Sponsoring Agency Code <b>ANM-110</b>	
15. Supplementary Notes					
16. Abstract <p>This report provides an overview of polymer flammability from a materials science perspective and describes currently accepted test methods to quantify burning behavior. Simplifying assumptions about the gas and condensed phase processes of flaming combustion provide mathematical relationships between polymer properties, chemical structure, flame resistance, and fire behavior that can be used to design fire-resistant plastics.</p>					
17. Key Words <b>Polymer, Plastic, Flammability, Heat release rate, Flame, Fire, Combustion</b>			18. Distribution Statement <b>This document is available to the public through the National Technical Information Service (NTIS) Springfield, Virginia 22161.</b>		
19. Security Classif. (of this report) <b>Unclassified</b>		20. Security Classif. (of this page) <b>Unclassified</b>		21. No. of Pages <b>82</b>	22. Price

## ACKNOWLEDGEMENTS

This work is dedicated to the memory of Dr. Thor I. Eklund, former FAA Branch Manager for Fire Research, whose vision and efforts made this report possible.

## TABLE OF CONTENTS

	Page
EXECUTIVE SUMMARY	xiii
1. INTRODUCTION	1
2. THE BURNING PROCESS	2
2.1 The Gas Phase	3
2.1.1 Kinetics	3
2.1.2 Thermochemistry	5
2.1.3 Energetics	6
2.2 The Mesophase	7
2.2.1 Kinetics	9
2.2.2 Thermochemistry	12
2.2.3 Energetics	14
2.3 The Condensed Phase	15
3. FIRE BEHAVIOR OF SOLID POLYMERS	17
3.1 Ignition	17
3.1.1 Chemical Criteria	18
3.1.2 Thermal Criterion	20
3.2 Steady Burning	22
3.3 Unsteady Burning	24
4. CHEMICAL STRUCTURE AND FIRE PROPERTIES	27
4.1 Heat Transport	28
4.2 Heat of Combustion	28
4.3 Enthalpy of Gasification	29
4.4 Ignition Temperature	30
4.5 Char Yield	34
4.6 Heat Release Rate	35
4.7 Flame Resistance	38
4.8 Smoke	40
5. FIRE AND FLAMMABILITY TESTS	42

5.1	Terminology: Fire Versus Flammability	42
5.2	Fire and Flammability Test Applications	43
5.2.1	Regulatory Compliance	43
5.2.2	Quality Assurance and Research	43
5.2.3	Data for Fire Safety Engineering Design and Analysis	43
5.3	Fire and Flammability Test Standards	44
5.3.1	Consensus-Based Test Standards	44
5.3.2	Other Types of Test Standards	45
5.4	Testing for Regulatory Compliance	45
5.4.1	Typical Example of a Flammability Test	46
5.4.2	Typical Examples of Fire Tests	47
5.5	Testing for Quality Assurance and Research	50
5.5.1	The LOI Test	50
5.5.2	The Pyrolysis Combustion Flow Calorimeter	51
5.6	Testing to Obtain Engineering Data	51
5.6.1	Bench-Scale Calorimeters	51
5.6.2	Large-Scale Calorimeters	54
6.	REFERENCES	56
APPENDIX A—TABULAR DATA FOR POLYMERS		

## LIST OF FIGURES

Figure		Page
1	Heat Release Capacity, Cost, and Flame Resistance of Commercial Polymers	1
2	Physical and Chemical Processes in the Flaming Combustion of Polymers	3
3	Gas Phase Kinetics: Accelerating ( $f > g$ ), Steady Growth ( $f = g$ ), and Steady-State ( $f < g$ ) Radical Concentration Histories at Ignition	5
4	Mesophase Profiles of Temperature, Viscosity, and Density During Flaming Combustion	8
5	Phenomenology of Polymer Burning	8
6	Fractional Mass Loss Rate Versus Temperature for Polybenzimidazole in TGA ( $\beta = 10$ K/min)	9
7	Char Mass Fraction in Fire Versus Anaerobic Pyrolysis	11
8	Thermogravimetric Analysis Data for PMMA and PAI (a) Residual Mass Fraction Versus Temperature and (b) Mass Loss Rate Versus Temperature	13
9	Char Mass Fraction Versus Hydrogen Mole Fraction in Polymer	14
10	Temperature Dependence of Polymer Heat Capacity, Thermal Conductivity, and Density	16
11	Ignition Temperature Versus External Heat Flux for PPS, PC, PA6, PBT, PS, PP, UPT, and PMMA	21
12	Critical Heat Flux Versus Ignition Temperature	22
13	Representative HRR Histories in Flaming Combustion for Thick and Thin Samples of Charring and Noncharring Polymers	23
14	Average HRR in Flaming Combustion Versus Char Yield of Polymers	24
15	Heat Release Rate Versus External Heat Flux Data for PA6 From Different Sources	25
16	Ignition/Fire Point Temperature Versus Decomposition/Flash Point Temperature for Solid and Liquid Fuels	32
17	Pyrolysis Temperature Versus Activation Energy of Polymers	33
18	Average HRR Versus Heat Release Capacity of Polymers	36

19	Polymer Heat Release Capacities: Calculated Versus Measured Values	38
20	Flammability Rating in UL 94 Test Versus Heat Release Capacity of 50 Polymers	39
21	Limiting Oxygen Index Versus Heat Release Capacity for 50 Polymers	40
22	Smoke Extinction Area Versus Flaming Combustion Efficiency ( $\chi$ ) for 40 Polymers	41
23	UL 94 Cabinet	46
24	The Steiner Tunnel Test Apparatus	47
25	The Radiant Flooring Panel Test Apparatus	48
26	Rate of Heat Release Apparatus	49
27	The LOI Test Apparatus	50
28	Commercial Version of the Cone Calorimeter	52
29	Commercial Version of the Fire Propagation Apparatus	53
30	ISO 9705 Room/Corner Test in Progress	55



## LIST OF TABLES

Table		Page
1	Components of the Enthalpy of Gasification for PMMA, PS, and PE	15
2	Mass Loss Rate, Effective HOC, and HRR at Ignition (Flash Point) and Incipient Burning/Extinction (Fire Point)	18
3	Heats of Gasification, Pyrolysis Activation Energy, Char Yield, as Well as Calculated and Measured Molecular Weights of Decomposition Products for Some Polymers.	30
4	Thermokinetic Properties of PMMA, PE, and Phenolic Triazine	31
5	Group Contributions to the Decomposition Temperature of Polybenzimidazole	34
6	Group Contributions to the Char Yield of Bisphenol-A Polycarbonate	35
7	Group Contributions to the Heat Release Capacity of PET	38
8	UL 94 20-mm Vertical Burning Test Classification Criteria	39

## LIST OF ACRONYMS

ABS	Acrylonitrile-butadiene-styrene terpolymer
C/H	Carbon/hydrogen
CFR	Code of Federal Regulations
CHF	Critical heat flux
EP	Epoxy
FSI	Flame spread index
H	Horizontal test
HOC	Heat of combustion
HRP	Heat release parameter
HRR	Heat release rate
ICAL	Intermediate-Scale Calorimeter
IEC	International Electrotechnical Committee
ISO	International Organization for Standardization
LFL	Lower flammability limit
LOI	Limiting oxygen index
MMA	Methylmethacrylate
MW	Megawatt
NBS	National Bureau of Standards
NFPA	National Fire Protection Association
PA	polyamides
PA6	Polycaprolactam
PAI	Polyamideimide
PBI	2,2'-m-phenylene-5,5'-bibenzimidazole
PBT	Polybutylene-terephthalate
PC	Polycarbonate
PCFC	Pyrolysis combustion flow calorimeter
PE	Polyethylene
PEEK	Polyetheretherketone
PEI	Polyetherimide
PES	Polyethersufone
PET	Polyethyleneterephthalate
PMMA	Polymethylmethacrylate
POM	Polyoxymethylene
PP	Polypropylene
PPO	Polyphenyleneoxide
PPS	Polyphenylenesulfide
PS	Polystyrene
PSU	Polysufone
PVC	Polyvinylchloride
RMD	Reactive molecular dynamics
SDI	Smoke-developed index
SEA	Smoke extinction area
TGA	Thermogravimetric analyzer
T <sub>ign</sub>	Ignition temperature

$t_{\text{ign}}$	Time to ignition
TRP	Thermal response parameter
UL	Underwriters Laboratory
UPT	Unsaturated polyester thermoset resin
V	Vertical test
VE	Vinyl Ester

## EXECUTIVE SUMMARY

This report provides an overview of polymer flammability from a materials science perspective and describes currently accepted test methods to quantify burning behavior. Simplifying assumptions about the gas and condensed phase processes of flaming combustion provide mathematical relationships between polymer properties, chemical structure, flame resistance, and fire behavior that can be used to design fire-resistant plastics.

## 1. INTRODUCTION.

Plastics (polymers) are a large and growing fraction of the fire load in homes, commercial environments, and transportation [1-5]. Moreover, the plastics that are most widely used are the least expensive and tend to be the most flammable. Flammability, which generally refers to the propensity of a substance to ignite easily and burn rapidly with a flame, is one indicator of fire hazard. Figure 1 shows the relationship between two measures of flammability: heat release capacity (section 4.6) and flame resistance (section 5.4) versus the truckload price of commercial polymers. Flammability and cost span over two orders of magnitude. The commodity polymers costing less than about \$1/pound comprise over 95% of the polymers in use, and these will continue to burn after brief exposure to a small flame. Engineering and specialty plastics costing over \$2/pound are typically polymers with aromatic backbones and fluoropolymers, which self-extinguish or resist ignition because of high thermal stability or low fuel value. Figure 1 shows that the flame resistance of polymers does not always correlate with cost but does correlate reasonably well with heat release capacity.

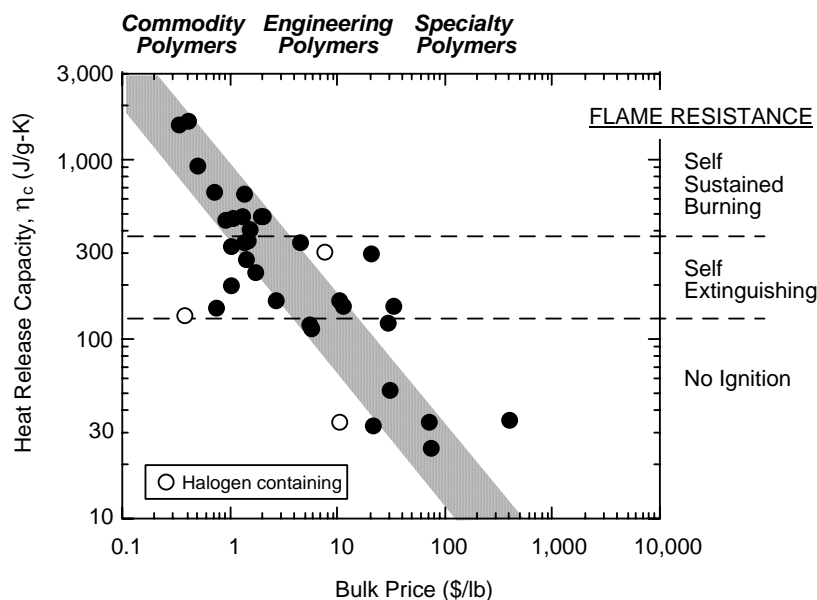


FIGURE 1. HEAT RELEASE CAPACITY, COST, AND FLAME RESISTANCE OF COMMERCIAL POLYMERS

Regulations [1 and 5] governing the flammability of plastics (e.g., section 5.4) used in consumer electronics, electrical equipment, building and construction, home furnishings, automobiles, and public transportation have created an annual worldwide market of tens of billions of pounds for flame-retardant plastics [1]. The designations flame-retardant, flame resistant, or ignition resistant as it applies to these plastics typically refer to the tendency of a thin (2- to 3-mm) strip of the material to withstand a brief exposure to a Bunsen burner flame or a hot wire without continuing to burn. Flame or ignition resistance is a low level of fire safety that is intrinsic to heat-resistant polymers but can be achieved with commodity polymers by adding flame-retardant chemicals [1-4]. The economic incentive to add flame-retardants to commodity polymers to pass flammability requirements (i.e., the slope in figure 1) has focused polymer flammability research

over the past few decades on the mechanisms and efficacy of flame-retardant additives [6-10], rather than on polymer flammability as an intrinsic material property. This trend in research, combined with the fact that flaming combustion of solids is a highly coupled, multiphased process and that fire test results depend on the apparatus, test conditions, and sample geometry, has limited the understanding of polymer flammability to a descriptive and qualitative nature.

In this report, simplifying assumptions were made about the burning processes under well-defined (standardized) conditions to provide mathematical relationships between polymer chemical structure and flammability properties. Experimental data was used in lieu of, and in support of, analytic results drawn from the broad subject material that is listed in the references. The goal of this report was to provide a consistent, mechanistic interpretation of the burning process as it relates to synthetic polymers and to describe currently accepted test methods to quantify burning behavior.

## 2. THE BURNING PROCESS.

Gases and volatile liquids are small molecules that are held together by weak ( $< 1$  kJ/kg) secondary chemical bonds. These volatile compounds spontaneously form combustible mixtures with air that ignite easily and burn with a high velocity. Polymers are very large (macro) molecules with the same intermolecular and intramolecular forces as low molecular weight compounds, but their boiling temperature is essentially infinite because of their high molecular weight. Consequently, both intermolecular and intramolecular (backbone) chemical bonds of polymers must be broken to generate volatile fuel species. This process requires a large ( $\approx 2$  MJ/kg) and continuous supply of thermal energy for ignition and sustained burning.

Flaming combustion can be roughly divided into physical and chemical processes taking place in each of three separate phases: gas, mesophase, and condensed (liquid/solid) phase [6,7, and 10-16]. The mesophase is the interface between the gas and condensed phase during burning. Figure 2 shows a schematic diagram of a horizontal polymer slab that is burning with a diffusion flame. The physical processes are shown on the left-hand side of figure 2, which include (1) energy transport by radiation and convection between the gas phase (flame) and the mesophase and (2) energy loss from the mesophase by mass transfer (vaporization of the pyrolysis gases) and conduction into the solid. At typical burning rates, the polymer surface (mesophase) recedes at a velocity of about  $10^{-6}$  m/s. Conservation of momentum at the gas-mesophase boundary shows that fuel gases evolve at a relatively low velocity ( $\approx 10^{-3}$  m/s) compared to the burning velocity of these gases when mixed with air ( $\approx 1$  m/s). Consequently, fuel generation is the rate-limiting step in polymer flaming combustion, and it is governed primarily by the rate at which heat and mass are transported to and from the polymer, respectively.

The important chemical processes are shown on the right-hand side of figure 2, which include (1) thermal degradation of the polymer in a thin surface layer (the mesophase) as a consequence of the physical (energy transport) processes, (2) mixing of the volatile pyrolysis products with air by diffusion, and (3) combustion of the fuel-air mixture in a combustion zone that produces radiant energy over a spectrum of wavelengths including visible. The combustion zone is bounded by a fuel-rich region on the inside and a fuel-lean region on the outside. Increasing the concentration of oxygen in the environment is known to increase the flame heat flux, either due

to a higher flame temperature, an increase in the volume of the combustion zone, or an increase in the soot concentration (luminosity) of the flame. The chemical and physical processes of flaming combustion particular to each of the gas, meso, and solid phases are treated separately below.

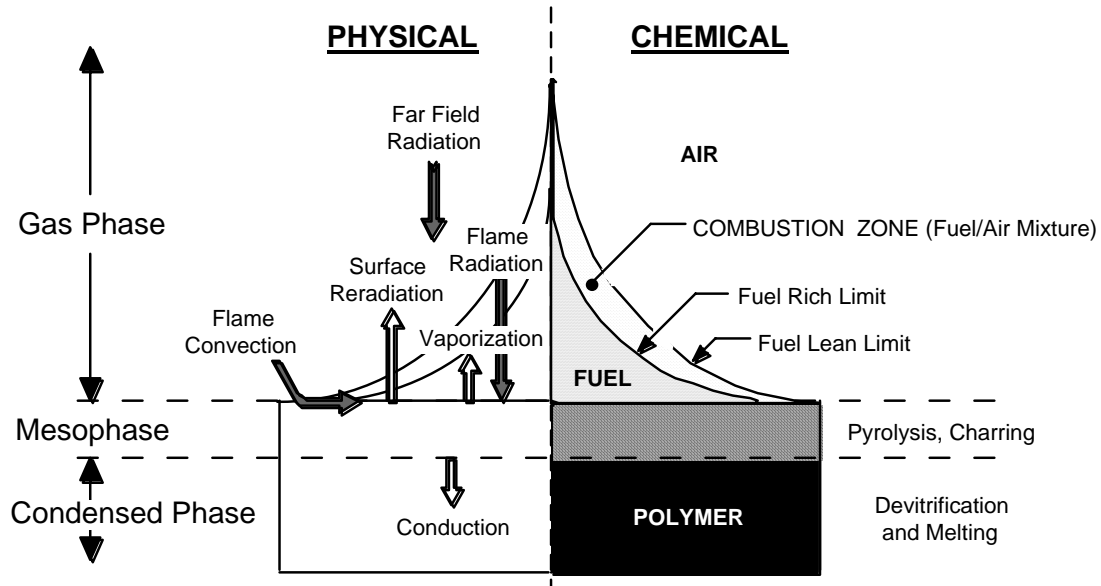
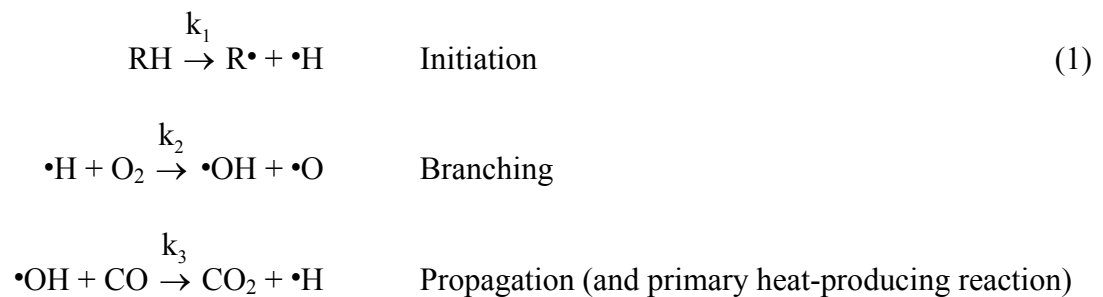


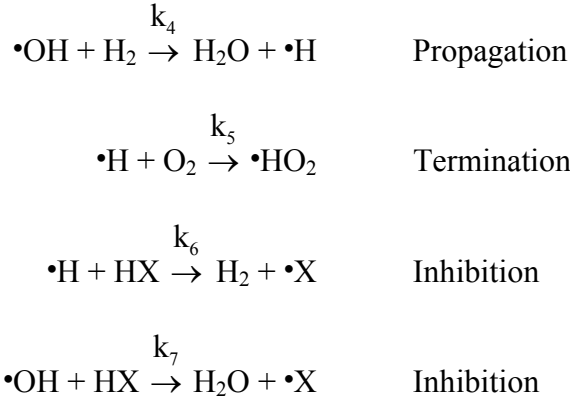
FIGURE 2. PHYSICAL AND CHEMICAL PROCESSES IN THE FLAMING COMBUSTION OF POLYMERS

## 2.1 THE GAS PHASE.

### 2.1.1 Kinetics.

Condensed phases (solids and liquids) of combustible compounds will only burn if they can be made to generate a volatile fuel and air mixture; therefore, the phenomena that led to ignition and the release of heat are those of the gas phase [11-19]. Although there are hundreds or thousands of chemical reactions going on in the flame that convert oxygen and fuel to stable combustion products, kinetic modeling and experimental data have shown that the burning velocity is most sensitive to the following reactions involving active radicals (denoted by  $\bullet$ ) of fuel (R), hydroxyl (OH), hydrogen (H), and oxygen (O), and halogen or phosphorus (X) are





The set of seven radical reactions in equation 1 accounts for the key processes of initiation, branching, propagation, and termination typical of hydrocarbon fuels as well as the inhibition reactions that are important for polymers containing halogen or phosphorus in a low oxidation state. Because the concentrations of radicals are empirically related as  $[\text{H}] \approx [\text{OH}] \approx 2[\text{O}]$ , the set of equations can be solved for the total concentration of active radicals:  $[\text{n}] = [\text{H}] + [\text{O}] + [\text{OH}]$ . Defining a rate of chain initiation,  $\theta = k_1[\text{RH}]$ , a branching coefficient  $f = 2/5 k_2[\text{O}_2]$ , and a linear termination coefficient,  $g = 2/5 \{k_5[\text{O}_2] + (k_6+k_7)[\text{HX}]\}$ , the rate of change of radical concentration at time,  $t$ , is

$$\frac{d[\text{n}]}{dt} = \theta + f[\text{n}] - g[\text{n}] \quad (2)$$

The general solution of equation 2 for the total radical concentration at any time is

$$[\text{n}] = \frac{\theta}{g-f} (1 - e^{-(g-f)t}) \quad (3)$$

Figure 3 shows a plot of equation 3 for three special cases:

- $f > g$ : In this case, the branching reactions dominate and the radical concentration increases exponentially as  $[\text{n}] = (\theta \exp[(f-g)t] - 1)/(f-g)$ , until the reactants are depleted.
- $g = f$ : In this case, the radical concentration increases steadily with time as  $[\text{n}] = \theta t$ , which is the boundary between steady state and exponential growth.
- $g > f$ : In this case, the rate of chain termination is greater than branching, and a steady-state concentration is reached at  $[\text{n}] = \theta/(g-f)$ . This steady state may be above or below the concentration for flame propagation.

The molar inhibition efficiency of the halogen atoms  $\text{X} = \text{bromine (Br), chlorine (Cl), and fluorine (F)}$  is found to be in the ratio  $\text{Br/Cl/F} = 10/2/1$ , i.e., bromine is ten times more efficient than fluorine and five times more efficient than chlorine on a mole basis. On a mass basis, the inhibitor efficiency is  $\text{Br/Cl/F} = 2/1/1$ , which explains the widespread use of bromine-containing monomers and additives as flame-retardants [4-10].



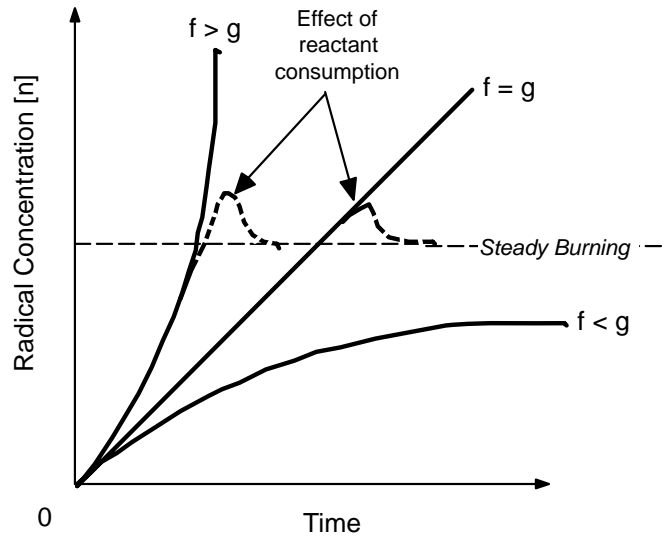
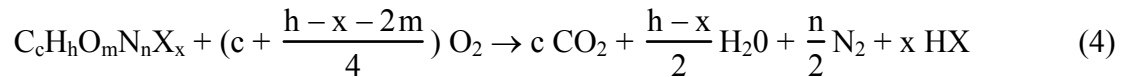


FIGURE 3. GAS PHASE KINETICS: ACCELERATING ( $f > g$ ), STEADY GROWTH ( $f = g$ ), AND STEADY-STATE ( $f < g$ ) RADICAL CONCENTRATION HISTORIES AT IGNITION

### 2.1.2 Thermochemistry.

If the kinetics are such that the combustion reactions proceed to completion at a rate that sustains flaming combustion, the chemical reaction of a generic fuel with atmospheric oxygen yields carbon dioxide ( $\text{CO}_2$ ), water ( $\text{H}_2\text{O}$ ), nitrogen ( $\text{N}_2$ ), and mineral acid ( $\text{HX}$ ) in quantitative yield:



Equation 4 assumes complete, 100% efficient, conversion of reactants (fuel gases and  $\text{O}_2$ ) to products ( $\text{CO}_2$  and  $\text{H}_2\text{O}$ ). Flaming combustion efficiency rarely exceeds 99% and typically ranges from 50% to 95%. Smoke is a combination of complete ( $\text{CO}_2$ ,  $\text{H}_2\text{O}$ , and acid gases) and incomplete (soot, carbon monoxide, and partially oxidized fuel gases) combustion products that occurs when combustion inhibitors are present, oxygen concentration is low, or there is insufficient reaction time or temperature in the combustion zone. The composition of smoke is highly dependent on the chemical composition of the polymer and the ventilation conditions under which the polymer is burning. Acid gases are irritating to the eyes and nasal passages, which makes escape more difficult. Carbon monoxide is the primary toxic compound in smoke. Soot absorbs light, which limits visibility and increases the luminosity or radiant power of the fire. Smoke is considered to be the main fire hazard but it depends on ventilation and the burning rate of the polymer; therefore, it is the latter quantity, i.e., the burning or heat release rate (HRR), that is considered to be the primary indicator of a fire hazard [4, 11, 12, 20, and 21].

The chemical pathway to soot formation is a recombination of aromatic radical fragments in the fuel-rich region inside the flame (see figure 2). Minute (10-100 nm in diameter) polycyclic, aromatic hydrocarbon particles are formed. These elementary soot particles may oxidize in the combustion zone of the flame. However, the elementary soot particles will agglomerate and grow in size until they are large enough to interact with visible light (0.3-0.7  $\mu\text{m}$ ), ultimately

reaching sizes on the order of a micron that absorb infrared radiation. Smoke is a combination of these soot particles in an aerosol with unburned liquid hydrocarbons, carbon dioxide/monoxide, water, and halogen acid gases, if present in the burning polymer [11-13].

### 2.1.3 Energetics.

Regardless of the gas phase combustion kinetics and thermochemistry, burning will only be possible if the energy balance is favorable. The first law of thermodynamics for a constant pressure gas phase process in which all of the work is pressure-volume work states that the internal energy change,  $dU$ , is related to the change in heat content,  $dQ$ .

$$dU + PdV = dQ \quad (5)$$

If the volatile fuel and air are well-mixed and react to generate a power density  $\dot{Q}'''$  (heat of combustion per unit volume per unit time,  $W/m^3$ ), a portion of which accumulates in the reaction volume as a rise in the temperature of the fuel-air mixture and a portion of which is lost to the surroundings at ambient temperature,  $T_a$ , by convection and radiation, the first law energy balance for the fuel-air mixture during deflagration (burning) is

$$\rho c \frac{dT}{dt} + P \frac{dV}{V} = \dot{Q}''' - \frac{\bar{h}S}{V}(T - T_a) - \frac{\varepsilon\sigma S}{V}(T^4 - T_a^4) \quad (6)$$

where  $\rho$ ,  $c$ ,  $V$ , and  $T$  are the instantaneous density, heat capacity, volume, and temperature of the fuel/combustion products/air mixture,  $\bar{h}$  is the average heat transfer coefficient at the boundary between the combustible mixture and the environment having surface area,  $S$ , at temperature,  $T$ , and pressure,  $P$ . In equation 6,  $\varepsilon$  is the gas emissivity and  $\sigma$  is the Stefan-Boltzmann constant. Defining quantities:  $\theta = T - T_a$ ,  $\tau = \rho c V / \bar{h} S$ , and assuming a constant fraction,  $\phi$ , of the power density is lost by radiation to the surroundings.

$$\frac{S}{V} \varepsilon \sigma (T^4 - T_a^4) \approx \phi \dot{Q}''' \quad (7)$$

Substituting equation 7 into equation 6, rearranging, and separating variables

$$\frac{d\theta}{dt} - \frac{\theta}{\tau} = \frac{1}{\rho c} \left[ \dot{Q}'''(1 - \phi) - P \ln V \right] \quad (8)$$

where  $\dot{Q}'''$ ,  $\rho$ , and  $c$  are initial values for the mixture. If deflagration (burning) raises the temperature from  $T_a$  to  $T_f$  with a corresponding increase in volume from  $V_a$  to  $V_f$  at constant pressure over a short time interval  $(0, t_f)$  with  $t_f \ll \tau$  and heat is transferred by radiation only, equation 8 becomes

$$T_f - T_a \approx \frac{1}{\rho c} \left( \dot{Q}'''(1 - \phi) - P \ln \left[ \frac{V_f}{V_a} \right] \right) \quad (9)$$

where  $Q''' = t_f \dot{Q}'''$  (J/m<sup>3</sup>) is the energy density at ignition. If the moles of reactants (fuel and air) and combustion products (CO<sub>2</sub> and H<sub>2</sub>O, principally) are equal and behave as ideal gases, and  $T_f$  is the (quasi) adiabatic flame temperature

$$Q''' = \frac{\rho c(T_f - T_a) + P \ln[T_f/T_a]}{1 - \phi} \quad (10)$$

The lower flammability limit (LFL) is the minimum volume (or mole) fraction of fuel in a fuel-air mixture that sustains ignition [11, 12, and 18]. The LFL has been measured for hundreds of gaseous and liquid hydrocarbon fuels, including fuels that contain oxygen, nitrogen, sulfur, boron, phosphorus, and halogen [11]. The average value of  $Q'''$  for 236 combustible compounds is

$$Q''' = \rho_f h_c^0 \text{LFL} = 1864 \pm 278 \frac{\text{kJ}}{\text{m}^3} \quad (11)$$

where  $\rho_f$  and  $h_c^0$  are the vapor density and heat of complete combustion of the fuel, respectively. If burning occurs at the LFL of the fuel, then equations 10 and 11 are equal and

$$\frac{\rho c(T_f - T_a) + P \ln[T_f/T_a]}{1 - \phi} = 1.9 \frac{\text{MJ}}{\text{m}^3} \quad (12)$$

Equation 12 can be solved for the quasi-adiabatic flame temperature at standard temperature and pressure. For  $\phi < 0.2$ , the calculated flame temperatures using equation 12 are in the range  $T_f = 1720 \text{ K} - 1420 \text{ K}$ , compared to experimental values  $T_f = 1600 \pm 100 \text{ K}$  [11 and 12]. Equation 12 shows that the LFL corresponds to a temperature  $T_f \approx 1600 \text{ K}$  at which the rate of heat losses from the flame equal the rate of heat production in the flame due to the combustion reactions.

## 2.2 THE MESOPHASE.

The mesophase is the interface between the gas and condensed phases during burning. All the thermal degradation chemistry that results in volatile fuel generation occurs in the mesophase (also known as the pyrolysis zone). A qualitative diagram of the mesophase properties is shown in figure 4. The temperature distribution at the burning surface is primarily a consequence of the prevailing energy balance but the viscosity, density, and physical dimension of the mesophase shown qualitatively in figure 4 are determined by the temperature field and thermal degradation chemistry. For polymers that thermally degrade with the formation of a solid char, the viscosity of the mesophase is higher than the molten polymer and probably comparable to the solid polymer. The mesophase is comprised of thermal degradation products in a variety of phases, including gas, liquid, and solid, as indicated in figure 4 by the bubble density and in figure 5 by a generic product distribution.

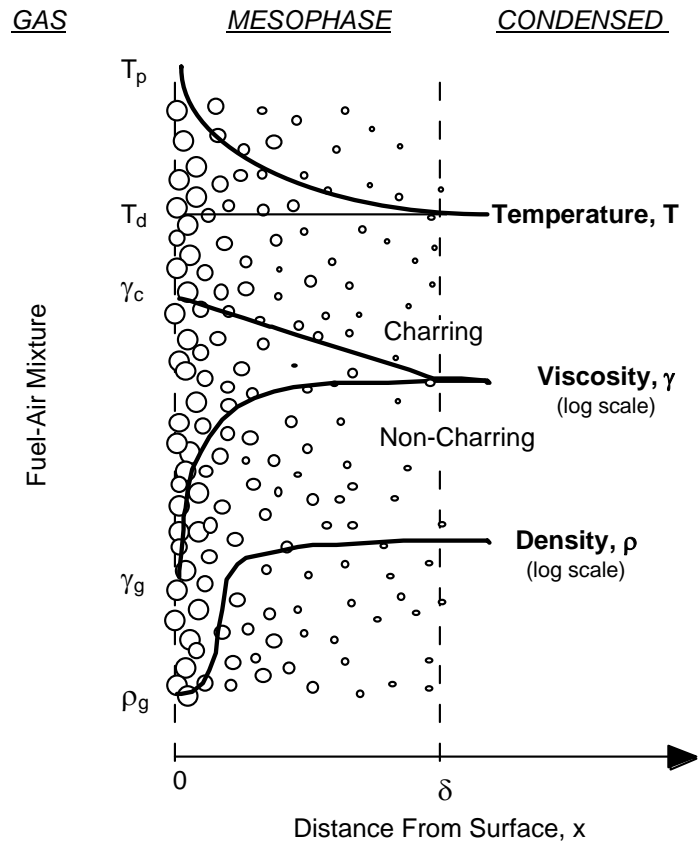


FIGURE 4. MESOPHASE PROFILES OF TEMPERATURE, VISCOSITY, AND DENSITY DURING FLAMING COMBUSTION

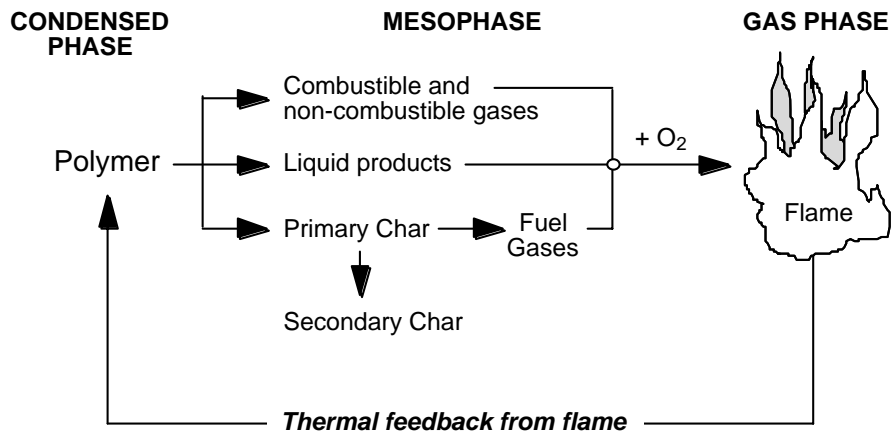


FIGURE 5. PHENOMENOLOGY OF POLYMER BURNING

Figure 5 shows the phenomenology of polymer burning and illustrates the coupled nature of the flaming combustion of condensed phases. The sequence of events for self-sustained burning involves the application of heat sufficient to thermally degrade (pyrolyze) the solid polymer to a

low molecular weight volatile fuel species and possibly a nonvolatile/solid char, depending on the polymer chemical structure. Mixing of the volatile thermal degradation products with atmospheric oxygen and ignition of this fuel and air mixture results in flaming combustion. Flaming combustion produces thermal energy in proportion to the heat of combustion of the volatile thermal degradation products and at a rate that is controlled by the fuel generation rate. The majority of the combustion energy from the flame is lost to the environment, but a fraction is returned to the polymer surface by convection and radiation (see figure 2). If the feedback of thermal energy from the flame at the polymer surface is sufficient to generate fuel vapors, flaming combustion will continue after the ignition source is removed and burning will be self-sustained.

### 2.2.1 Kinetics.

In figure 5, the first stage of thermal degradation produces primary volatiles (gas and liquid products/tar) and possibly a primary char residue (see section 4.5). If a primary char forms, further decomposition generates a secondary gas (principally hydrogen) and a thermally stable carbonaceous char. Figure 6 shows thermogravimetric analyzer (TGA) data at a heating rate of 10 K/min for anaerobic pyrolysis of polybenzimidazole (2,2'-(m-phenylene)-5,5'-bibenzimidazole). Polybenzimidazole is a heat-resistant, char-forming polymer that thermally degrades by primary and secondary decomposition events, as evidenced by the distinct mass loss rate peaks for these processes. Models have been proposed that account for some or all of the pyrolysis products (gas, tar, primary char, secondary char, and secondary gas) as various combinations of sequential or simultaneous thermal degradation reactions. However, a detailed mechanism for the thermal degradation of most polymers, especially char-forming polymers, is unlikely and unnecessary for a phenomenological treatment of fuel generation chemistry.

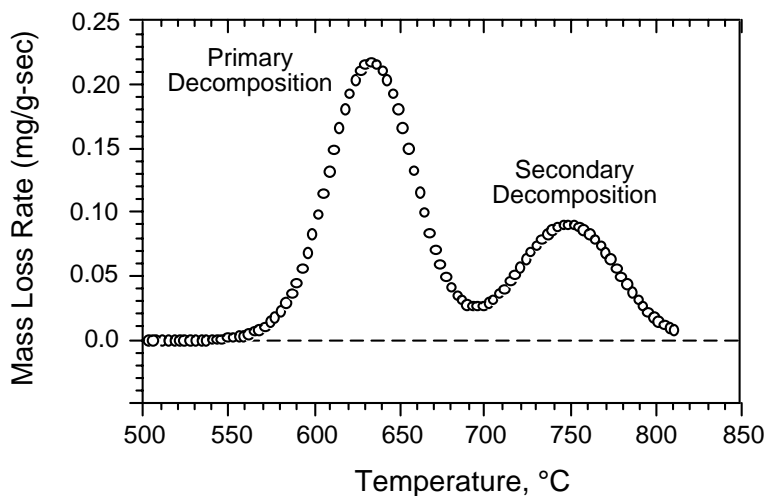
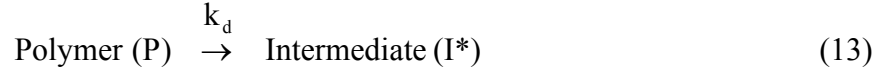


FIGURE 6. FRACTIONAL MASS LOSS RATE VERSUS TEMPERATURE FOR POLYBENZIMIDAZOLE IN TGA ( $\beta = 10$  K/min)

Mechanistic reaction kinetics of polymer thermal degradation processes show that the overall mass loss (fuel generation) rate should be first order with respect to the instantaneous mass if the reactive intermediates (free radicals) maintain a steady-state concentration, regardless of whether

thermal degradation occurs by random or end-chain scission. A first-order thermal degradation scheme that accounts for the main pyrolysis products is [4, 7, and 10].



Equations 13-15 are a subset of the reactions shown in figure 5, but they are sufficient to represent the mesophase fuel generation kinetics. In particular, polymer P thermally degrades to a reactive intermediate I\* with rate constant  $k_d$ . The intermediate produces gas G and/or char C, with rate constants  $k_g$  and  $k_c$ , respectively. Figure 7 shows data for a variety of pure, unfilled polymers plotted as the mass fraction of char measured immediately after flaming combustion has ceased in a fire calorimeter (see section 5.6) versus the char residue at  $900 \pm 100^\circ\text{C}$  for the same material after anaerobic pyrolysis in a TGA at a heating rate of about 10 K/min. It is seen that the char yield of a material in a fire is essentially equal to its residual mass fraction after anaerobic pyrolysis at temperatures representative of the char temperature in a fire. Although oxidative degradation products have been identified at the surface of olefinic polymers after flaming combustion, the data in figure 7 suggest that oxidation reactions in the solid during flaming combustion are not important to the overall fuel fraction. If the reactive intermediate I\* in equations 13-15 is a stationary state, then  $dI^*/dt = 0$ , and if thermal decomposition is an anaerobic process, the fuel generation rate is

$$-\frac{dm'}{dt} = k_p m' = A e^{-E_a/RT} m' \quad (16)$$

where  $m'$  is the mass of volatile fuel,  $k_p$  is the mass loss rate constant in terms of a global frequency factor  $A$  (1/s) and activation energy  $E_a$  (J/mole). Equation 16 is easily solved for the fuel generation rate at constant temperature (isothermal conditions). However, the polymer temperature changes rapidly from ambient to the pyrolysis temperature near the burning surface; thus, a nonisothermal solution of equation 16 is required to capture the dynamics of the fuel generation process as it occurs in the mesophase. For an arbitrary temperature history  $T(t)$  in the mesophase, the mass of fuel generated at any time  $t$  is

$$\ln\left(\frac{m'(\tau\tau)}{m'(0)}\right) = -\int_0^t A \exp\left[-\frac{E_a}{RT(t')}\right] dt' \quad (17)$$

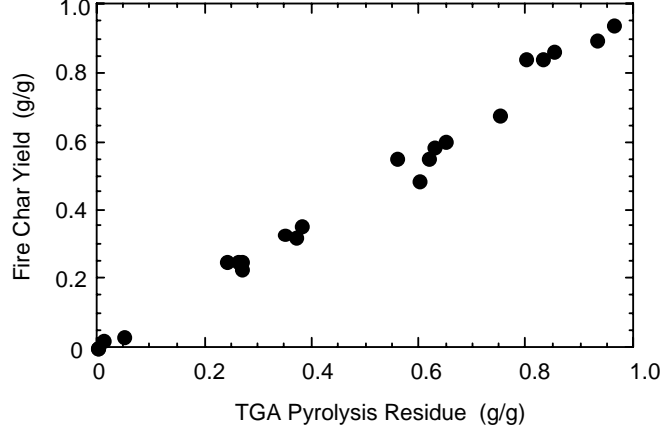


FIGURE 7. CHAR MASS FRACTION IN FIRE VERSUS ANAEROBIC PYROLYSIS

Equation 17 can be solved numerically for any specified temperature history. However, the mesophase temperature history is a function of both time and position (see figure 4); therefore, transient temperature distribution  $T(x,t)$  must be specified to obtain an analytic solution for equation 17. If the temperature distribution is static during steady burning of a thick sample as the surface  $x = 0$  recedes at constant velocity  $v = (dx/dt)_T$  and the mesophase is a thin surface layer, then the rate of temperature rise of the mesophase is constant,  $(dT/dt)_{x=0} = -v (dT/dx)_t = \beta$ . The assumption of a constant heating rate for the mesophase transforms the independent variable in equation 17 from time to temperature and allows for a solution in terms of the mass fraction of polymer remaining at temperature,  $T$ .

$$\frac{m(T)}{m_0} = \mu(T) + [1 - \mu(T)] e^{-y} \quad (18)$$

where

$$y = \frac{k_p RT^2}{\beta(E_a + 2RT)}$$

The equilibrium char fraction is

$$\mu(T) = \frac{k_c}{k_c + k_g} = \left[ 1 + \frac{A_g}{A_c} \exp\left(-\frac{E_g - E_c}{RT}\right) \right]^{-1} \quad (19)$$

in terms of the frequency factors,  $A_g$  and  $A_c$  and the activation energies  $E_g$  and  $E_c$ , for gas and char formation, respectively. A temperature-dependent equilibrium char fraction that is the ratio of rate constants for gas and char formation is consistent with the use of group contributions for the char-forming tendency of polymers [22] (see section 4.5). The fractional mass loss rate at temperature  $T$  is obtained by differentiating equation 18 with respect to time. For  $\mu(T) = \mu = \text{constant}$ , the result is

$$-\frac{1}{m_0} \frac{dm}{dt} = (1 - \mu) k_p e^{-y} \quad (20)$$

Setting the time derivative of equation 20 equal to zero shows that the maximum fuel generation rate occurs when

$$k_p(T_p) = A \exp\left[-\frac{E_a}{RT_p}\right] = \frac{\beta E_a}{RT_p^2} \quad (21)$$

Substituting  $k_p$  from equation 21 into equation 20 for  $E_a \gg RT_p$  gives the maximum fuel generation rate

$$-\frac{1}{m_0} \frac{dm}{dt} \Big|_{\max} = (1 - \mu) \frac{\beta E_a}{eRT_p^2} \quad (22)$$

The temperature  $T_p$  in equations 21 and 22 is the temperature at the maximum fuel generation rate during the course of the linear temperature history. Defining a characteristic heating rate,  $\beta^* = A \Delta T_p$  where  $\Delta T_p = RT_p^2/E_a$  is the half-width of the pyrolysis temperature interval, equation 22 takes the form of a (statistical) thermodynamic phase transition temperature.

$$T_p = \frac{E_a}{R \ln[\beta^*/\beta]} \quad (23)$$

TGA is a common laboratory method for studying the thermal degradation kinetics of polymers at a constant heating rate [6-10]. The maximum fuel generation rate and  $T_p$  are readily obtained from these experiments as shown in figure 8 for polymethylmethacrylate (PMMA) and polyamideimide (PAI). Figure 8 shows the onset thermal degradation temperature  $T_d$ , the temperature at peak mass loss rate  $T_p$ , and the char fraction  $\mu$  for PAI. The range of temperatures over which pyrolysis takes place is of the order  $eRT_p^2/(1-\mu)E_a$ , which is very different for these two polymers of widely differing thermal stability and charring tendency. Table A-1 in appendix A contains  $T_d$ ,  $T_p$ , and ignition temperatures for a number of polymers.

### 2.2.2 Thermochemistry.

The basic thermal degradation mechanism leading to volatile fuel generation in polymers involves primary and secondary decomposition events, as illustrated in figure 5. The primary decomposition step can be main-, end-, or side-chain scission of the polymer. Subsequent thermal degradation reactions depend largely on the chemical structure of the polymer but typically proceed by hydrogen transfer to  $\alpha$ - or  $\beta$ -carbons, nitrogen or oxygen, intramolecular exchange (cyclization), side-chain reactions, small-molecule ( $SO_2$ ,  $CO_2$ , and  $S_2$ ) elimination, molecular rearrangement, or unzipping to monomer [15]. Unzipping or depolymerization of vinyl polymers is characterized by a kinetic chain length or zip length that is the average number of monomer units produced by a decomposing radical before the radical is deactivated by termination or transfer. Mathematically, the zip length is the ratio of the rate constants for initiation to termination.



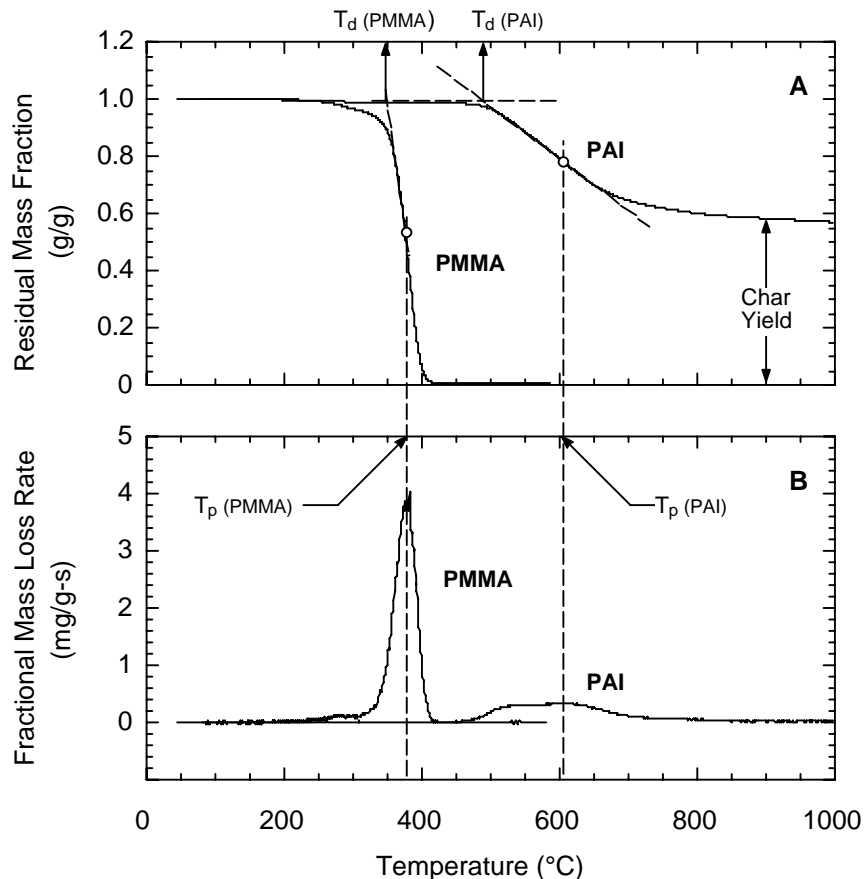


FIGURE 8. THERMOGRAVIMETRIC ANALYSIS DATA FOR PMMA AND PAI  
 (a) RESIDUAL MASS FRACTION VERSUS TEMPERATURE AND  
 (b) MASS LOSS RATE VERSUS TEMPERATURE

Aromatic backbone polymers such as polycarbonate, polyimides, polyaramides, polyarylsulfones, and polyphenyleneethers tend to decompose in varying degrees to a carbonaceous char residue through a complex set of intramolecular rearrangements and side-chain reactions involving cross-linking and bond scission. The char yield is the mass fraction of carbonaceous char that remains after flaming combustion of the polymer. Charring competes with termination reactions that generate volatile species, thus reducing the amount of available fuel in a fire. In addition, char acts as a heat and mass transfer barrier that lowers the flaming HRR. Figure 7 demonstrated that the char yield in a fire is roughly equal to the anaerobic pyrolysis residue at high (flame) temperatures. Polymers that contain heterocyclic or aromatic structures in the backbone tend to form char during thermal decomposition in rough proportion to the carbon/hydrogen (C/H) ratio of the polymer. Figure 9 shows the mass fraction of char plotted versus the mole fraction of hydrogen in the polymer molecule. High C/H ratios favor termination by crosslinking between carbon radicals and char is formed. Low C/H ratios favor termination of carbon radicals by hydrogen transfer, resulting in low molecular weight fuel species rather than char. The relative rates of intermolecular cross-linking and aromatization and intramolecular hydrogen transfer and cyclization reactions, i.e., the ratio  $k_c/(k_c+k_g)$  in equation 19, will determine the char yield at any particular hydrogen mole fraction.

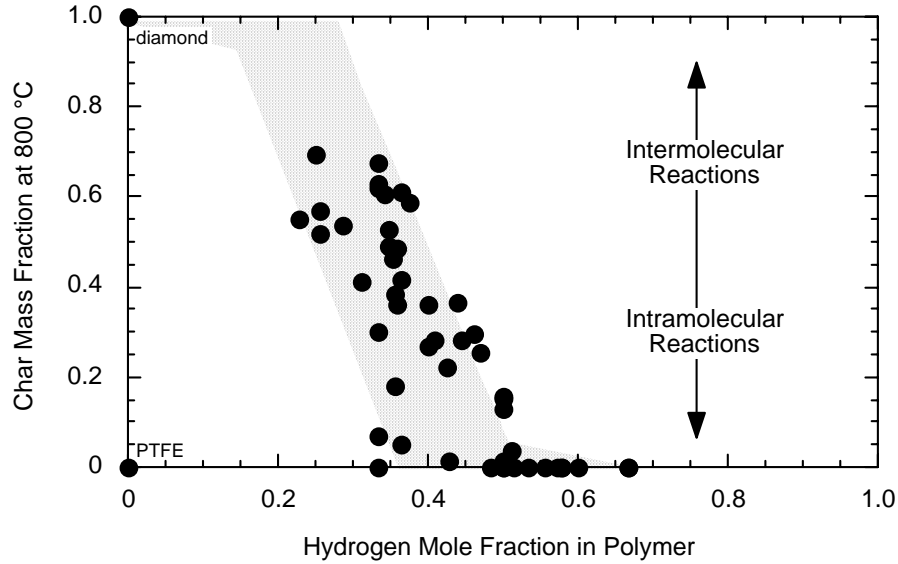


FIGURE 9. CHAR MASS FRACTION VERSUS HYDROGEN MOLE FRACTION IN POLYMER

### 2.2.3 Energetics.

In principle, the heat (enthalpy) of gasification is the difference between the enthalpy of the solid in the initial state at ambient temperature and pressure,  $T_0$  and  $P_0$ , and the enthalpy of the volatile thermal decomposition products at  $T_p$  and  $P_0$ . If the stored heat is  $\Delta h_s$ , the enthalpy of fusion (melting) for semicrystalline polymers is  $\Delta h_f$ , the bond dissociation enthalpy is  $\Delta h_d$ , and the enthalpy of vaporization of the decomposition products is  $\Delta h_v$ , then the enthalpy of gasification per unit mass of fuel is [10]

$$L_g = \Delta h_s + \Delta h_f + \Delta h_d + \Delta h_v = \int_{T_0}^{T_p} c(T)dT + \Delta h_f + \Delta h_d + \Delta h_v \quad (24)$$

The symbol  $L_g$  derives from latent heat, i.e., the recoverable heat in a reversible process. Thermolytic cleavage of primary chemical bonds in the polymer backbone to produce volatile fuel and char is obviously not a reversible process, but the symbol  $L_g$  will be used throughout to conform with the literature in the fire sciences. Table 1 illustrates the magnitude of these enthalpic terms for amorphous poly(methylmethacrylate), polystyrene, and semicrystalline polyethylene. The stored heat,  $\Delta h_s$ , was obtained by numerical integration of heat capacity versus temperature from ambient to the dissociation temperature as per equation 24. The dissociation (bond breaking) enthalpy,  $\Delta h_d$ , is assumed to be equal to the heat of polymerization but opposite in sign for these polymers, which thermally degrade by random or end-chain scission. The degradation product for polyethylene (PE) is assumed to be a tetramer (i.e., octane with  $M_g = 112$  g/mole) for the purpose of calculating the heats of dissociation and vaporization on a mass basis for this polymer, and the degree of polyethylene crystallinity of PE is taken to be 90%. All other enthalpies in table 1 were obtained from handbooks using monomer molecular

weights to convert the energies to a mass basis. The values for  $h_g$  in the second to last row were obtained by summing the individual enthalpies, according to equation 24, for each polymer.

TABLE 1. COMPONENTS OF THE ENTHALPY OF GASIFICATION FOR PMMA, PS, AND PE

	PMMA	PS	PE
Monomer MW (g/mole)	100	104	28
Fuel MW (g/mole)	100	104	112
$\Delta h_s$ (J/g)	740	813	803
$\Delta h_f$ (J/g)	amorphous	amorphous	243
$\Delta h_d$ (J/g)	550	644	910
$\Delta h_v$ (J/g)	375	387	345
$L_g = \sum \Delta h_i$ (J/g)	1665	1850	2301
$L_g$ (measured) J/g	1700	1800	2200

In practice, the enthalpy of gasification is rarely calculated because detailed and reliable thermodynamic data for the polymer and its decomposition products are generally unavailable. Direct laboratory measurement of  $L_g$  using differential thermal analysis and differential scanning calorimetry have been reported, but  $L_g$  is usually measured in a constant heat flux gasification device or fire calorimeter (see section 3.2). In these experiments, a plot of mass loss rate per unit surface area (mass flux) versus external heat flux has slope  $1/L_g$  where

$$L_g = \frac{h_g}{1-\mu} \quad (25)$$

$h_g$  is the heat of gasification per unit mass of solid and  $\mu$  is the nonfuel fraction (char or inert filler). The last row in table 1 lists the average of  $h_g$  values for these noncharring polymers. Agreement is quite good between experimental values and thermochemical calculations of  $h_g$ . Table A-2 in the appendix A contains  $L_g$ ,  $\mu$ , and  $h_g$  for 53 polymers. Analysis of the data in table A-2 shows that  $L_g$  and  $\mu$  vary widely with polymer chemical structure, but  $h_g$  is relatively independent of composition with an average value,  $h_g = 2.0 \pm 0.5$  kJ/g.

### 2.3 THE CONDENSED PHASE.

The rate at which heat is transported and stored in the condensed phase is of fundamental importance because these processes determine the time to ignition and burning rate of polymers. Table A-3 in the appendix A lists generic thermophysical properties at ambient temperature ( $295 \pm 3$  K) gathered from the literature for a number of common thermoplastics, thermoset resins, elastomers, and fiberglass-reinforced plastics [4]. Entries are individual values, averages of values from different sources, or averages of a range of values from a single source and, therefore, represent in most cases a generic property value with an uncertainty of about 10%-20%.

Neglecting changes in the slope or magnitude of thermal properties that occur at phase changes, such as the glass transition, melting, and decomposition temperatures of polymers, the temperature dependence of  $\kappa$ ,  $\rho$ , and  $c$  for an amorphous polymer can be roughly approximated

$$\kappa(T) = \kappa_0 \left[ \frac{T}{T_0} \right]^{\frac{1}{2}} \quad (26)$$

$$\rho(T) = \rho_0 \left[ \frac{T_0}{T} \right]^{\frac{1}{2}} \quad (27)$$

$$c(T) = c_0 \left[ \frac{T}{T_0} \right] \quad (28)$$

These properties are plotted in reduced form in figure 10 as  $P(T)/P(T_0)$  versus  $T/T_0$ , where  $P(T)$  and  $P(T_0)$  are the values of  $\kappa$ ,  $\rho$ , or  $c$  at temperature  $T$  and standard temperature (298 K), respectively.

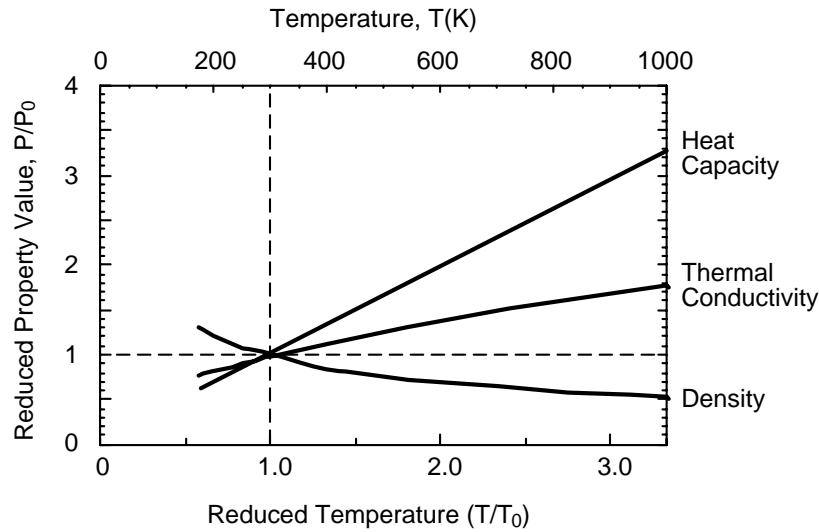


FIGURE 10. TEMPERATURE DEPENDENCE OF POLYMER HEAT CAPACITY, THERMAL CONDUCTIVITY, AND DENSITY

The product  $\kappa\rho c$  is a quantity called the thermal inertia that emerges from the transient heat transfer analysis of ignition time (see equation 40). The temperature dependence of  $\kappa$ ,  $\rho$ , and  $c$  in equations 26-28 suggest that the product of these terms (i.e., the thermal inertia) should have the approximate temperature dependence:

$$\kappa(T) \rho(T) c(T) \approx \kappa_0 \rho_0 c_0 T/T_0 = (\kappa\rho c)_0 T/T_0 \quad (29)$$

where  $\kappa_0$ ,  $\rho_0$ , and  $c_0$  are the room temperature ( $T_0$ ) values listed in appendix A table A-3.

Another thermal parameter that emerges from unsteady heat transfer analyses is the thermal diffusivity  $\alpha = \kappa/\rho c$ , which, according to equations 26-28, should be relatively independent of temperature

$$\alpha(T) = \frac{\kappa(T)}{\rho(T)c(T)} = \alpha_0 \quad (30)$$

Room temperature values of polymer thermal diffusivity are listed in appendix A table A-3.

Another thermal property that affects the response of a polymer to the exposure from an external heat source is the surface absorptivity. It is generally assumed that polymers behave as gray surfaces, i.e., the total hemispherical surface absorptivity is equal to the total hemispherical emissivity,  $\epsilon$ . Hallman [23] measured  $\epsilon$  for many polymers and different radiant heat sources. Some of Hallman's measurements are given in table A-4. These values are applicable prior to ignition, and it is reasonable to assume that  $\epsilon = 1$  for the flaming surface of a polymer.

### 3. FIRE BEHAVIOR OF SOLID POLYMERS.

The continuum level treatment of the fire behavior of polymers disregards the discrete (molecular) structure of matter so that the temperature distribution, and more importantly its derivatives, are continuous throughout the material. In addition, the polymer is assumed to be thermally thick and have identical properties at all points (homogeneous) and in all directions (isotropic). In this way, analytic results for ignition and burning can be derived from unsteady and steady heat transfer analyses, respectively, using simplified mass and energy balances. The continuum level treatment provides scaling relationships between the properties of polymers and their fire response but ignores many important characteristics of burning behavior, such as the effect of char formation on heat and mass transfer, swelling (intumescence), and dripping, that can only be captured empirically or through detailed numerical modeling and analyses.

#### 3.1 IGNITION.

Ignition is the initiation of combustion of a fuel-air mixture that is uniformly heated (autoignition) or comes in contact with a flame, spark, or glowing wire (piloted ignition). The ignition of volatile liquid and gaseous fuels is fairly well understood because only the global or local thermodynamic state of the system needs to be considered [11 and 17-19]. As shown in section 2.1, the reaction of gaseous fuels with air will be self-sustaining if the combustion energy density of the mixture is above a minimum (critical) value of about 2 MJ/m<sup>3</sup>. The burning of condensed phases is more complicated because there is dynamic coupling of heat and mass transfer between the gas phase and condensed (meso, solid) phase [11 and 12]. Consequently, a variety of criteria have been proposed for piloted ignition of solids, which can be roughly divided into thermal (condensed phase) and chemical (gas phase) [11 and 24]. The primary example of a thermal criterion is an ignition temperature for the solid, while chemical criteria extend to a critical mass flux or a critical HRR. Any of these criteria can be expressed in terms of an external heat flux at which the temperature or the flux of mass and energy reaches some critical value. The criteria for piloted ignition of polymer solids are examined separately below.

### 3.1.1 Chemical Criteria.

Chemical criteria for ignition of condensed phases include a boundary layer reaction rate and a critical mass flux of fuel gases, both of which are equivalent to establishing a LFL at the ignition source for a fixed test geometry and ventilation rate. Table 2 lists the mass fluxes at incipient piloted ignition and incipient burning or extinction for over 20 polymers measured in a fire calorimeter (section 5.6) or similar device. Also listed is the effective heat of combustion (HOC) of the fuel gases and the product of the mass flux and HOC at ignition or extinction, i.e., the HRR. The mass flux at ignition in table 2 varies between polymers because of differences in the LFL of their pyrolysis products or fuel gases. If piloted ignition occurs when the concentration of pyrolysis gases in air reaches the LFL of the particular fuel species and  $\dot{m}_f''$  and  $\dot{m}_a''$  are the mass fluxes of fuel and air in a well-mixed volume at the igniter, then for  $LFL \ll 1$ ,

$$\frac{\dot{m}_f''}{\dot{m}_a''} = \frac{m_f}{m_a} = \frac{\rho_f}{\rho_a} \left( \frac{LFL}{1-LFL} \right) \approx \frac{\rho_f}{\rho_a} LFL \quad (31)$$

The average convective heat transfer coefficient at the polymer surface at incipient ignition is

$$\bar{h} = c_a \dot{m}_a'' \quad (32)$$

The mass flux at ignition from equations 11, 31, and 32 is

$$\dot{m}_f''|_{LFL} = \frac{\rho_f}{\rho_a} \frac{\bar{h}}{c_a} LFL = \frac{\bar{h} Q''}{\rho_a c_a h_c^0} \frac{1}{h_c^0} = \frac{HRR^*}{h_c^0} \quad (33)$$

TABLE 2. MASS LOSS RATE, EFFECTIVE HOC, AND HRR AT IGNITION (FLASH POINT) AND INCIPIENT BURNING/EXTINCTION (FIRE POINT)

Polymer	HOC (kJ/g)	Flash Point		Fire Point	
		MLR (g/m <sup>2</sup> -s)	HRR (kW/m <sup>2</sup> )	MLR (g/m <sup>2</sup> -s)	HRR (kW/m <sup>2</sup> )
POM	14.4	0.88	13	1.7-4.5	40
PMMA	24.8	0.97-1.01	25	1.9-3.2	61
PE	40.3	0.88	35	1.3-2.5	73
PP	41.9	0.60	25	1.1-2.7	72
PS	27.9	0.57	16	0.8-4.0	50
PS FR	9.6	2.0	19	6-8	67
PUR	23.7	0.83	20	2.0	47
PA6	29.8	0.88	26	3.0	89
PBT	21.7	0.77	17	3.4	74
PC	21.2	0.78	17	3.4	72
PPS	23.5	0.81	19	3.6	85
PPZ	15.4	1.23	19	3.0	46

TABLE 2. MASS LOSS RATE, EFFECTIVE HOC, AND HRR AT IGNITION (FLASH POINT) AND INCIPIENT BURNING/EXTINCTION (FIRE POINT) (Continued)

Polymer	HOC (kJ/g)	Flash Point		Fire Point	
		MLR (g/m <sup>2</sup> -s)	HRR (kW/m <sup>2</sup> )	MLR (g/m <sup>2</sup> -s)	HRR (kW/m <sup>2</sup> )
PEN	22.9	0.71	16	2.7	62
PEEK	21.3	0.72	15	3.3	70
PESU	22.4	0.9	20	3.7	83
EP	21.3	1.0	21	3.4	72
CE	22.8	1.3	30	4.4	100
PBI	16.2	1.5	24	–	–
PI	12.0	1.30	16	4.0	48
PEI	16.7	0.82	14	–	–
PAI	19.3	1.63	31	2.5	48
Average:		1.0	21	3.2	66
Standard Deviation:		0.4	6	1.2	17

Equation 33 shows that there is a parameter with the units and significance of a virtual HRR,  $HRR^* = \bar{h}Q''' / \rho_a c_a$ , that is independent of the type of polymer but depends on the nature of the convective environment, i.e., the test conditions. Piloted ignition of a solid polymer will occur under a particular set of test conditions when

$$\dot{m}''_{ign} = \dot{m}''|_{LFL} \geq \frac{HRR^*}{h_c^0} \quad (34)$$

or when

$$h_c^0 \dot{m}''_{ign} \geq HRR^* \quad (35)$$

In fire calorimeters (section 5.6),  $HRR^*$  is of the order

$$HRR^* = \frac{\bar{h}Q'''}{\rho_a c_a} = \frac{(10 \text{ W/m}^2 - K)(1.9 \text{ MJ/kg})}{(1 \text{ kg/m}^3)(1 \text{ kJ/kg} - K)} \approx 20 \frac{\text{kW}}{\text{m}^2}$$

Equations 34 and 35 are physically based criteria for ignition of polymers in typical (section 5.6) convective environments where a spark is located 25 mm from the heated polymer surface. Equation 35 is a steady-state, two-dimensional analog of the combustion energy density criterion for gaseous ignition (equation 11) and, like that criterion, is independent of the chemical composition of the fuel gases. Using  $HRR^* = 20 \text{ kW/m}^2$  and the indicated HOC in table 2, equation 34 predicts  $\dot{m}''_{ign} = 1.00 \pm 0.37 \text{ g/m}^2\text{-s}$  at the flash point, which is indistinguishable from the average experimental result. Equation 35 predicts that piloted ignition is imminent when  $h_c^0 \dot{m}''_{ign} = HRR \geq HRR^* = 20 \text{ kW/m}^2$ , which is also indistinguishable from the experimental

result  $HRR = 21 \pm 6 \text{ kW/m}^2$  at incipient ignition (the flash point). Table 2 also lists the mass flux and HRR for the majority of polymers at the fire point when the flame is first established. The mass flux and HRR increase by a factor of 2-3 between the flash point and the fire point as additional heat flux is imparted to the surface from the flame at incipient burning.

### 3.1.2 Thermal Criterion.

A chemical criterion (equation 34 or 35) is probably sufficient for ignition to occur, but a surface temperature in the vicinity of the thermal decomposition temperature is necessary to begin the fuel generation process. The thermal theory of ignition assumes that the surface temperature at ignition is a characteristic property of the polymer. If fuel gasification obeys a simple energy balance, such as equation 24 and the temperature dependence of the heat capacity is equation 28, i.e.,  $c(T) = c_0 T/T_0$ , then the enthalpy of gasification at ignition is

$$\frac{c_0}{T_0} \int_{T_0}^{T_{\text{ign}}} T dT + \Delta h_f + \Delta h_d + \Delta h_v = L_g \quad (36)$$

The heat capacity-temperature integral in equation 36 can be solved explicitly with the result

$$\frac{c_0 T_{\text{ign}}^2}{2T_0} + \left( \Delta h_f + \Delta h_d + \Delta h_v - \frac{c_0 T_0}{2} \right) = L_g \quad (37)$$

The data in table 1 suggest that  $(\Delta h_f + \Delta h_d + \Delta h_v - c_0 T_0/2) \approx L_g/2$ , which allows equation 37 to be solved for ignition temperature,  $T_{\text{ign}}$ .

$$T_{\text{ign}} \approx \left[ \frac{T_0 L_g}{c_0} \right]^{1/2} \quad (38)$$

Figure 11 is a plot of measured surface temperature at piloted ignition in a fire calorimeter (section 5.6) or similar device over a range of external heat fluxes for polyphenylenesulfide (PPS), polycarbonate (PC), polycaprolactam (PA6), polystyrene (PS), polybutylene-terephthalate (PBT), polypropylene (PP), unsaturated polyester thermoset (UPT), and PMMA. The ignition temperature of each polymer is relatively independent of heat flux, per equation 38, which also accounts for the large differences between polymers (see table A-1). Using typical properties for commodity and engineering polymers

$$T_{\text{ign}} = \left[ \frac{T_0 L_g}{c_0} \right]^{1/2} = \left[ \frac{(298\text{K})(2\text{MJ/kg})}{1.5\text{kJ/kg-K}} \right]^{1/2} = 630\text{K} = 357^\circ\text{C}$$

which approximates the ignition temperature of these materials in the lower part of figure 11. For a constant ignition temperature, unsteady heat transfer [4, 11, and 12] gives the time to ignition,  $t_{\text{ign}}$ , for a thermally thick sample at a constant external heat flux,  $\dot{q}_{\text{ext}}''$



$$\frac{1}{\sqrt{t_{\text{ign}}}} = \frac{\dot{q}_{\text{ext}}'' - \dot{q}_{\text{loss}}''}{\text{TRP}} \quad (39)$$

where

$$\text{TRP} = \frac{\sqrt{\pi\kappa\rho c}}{2} (T_{\text{ign}} - T_0) \quad (40)$$

is a quantity known as the thermal response parameter (TRP). Equation 39 states that a plot of the reciprocal square root of the time to ignition versus the external heat flux has a slope equal to the average value of the thermal response parameter. The product  $\kappa\rho c$  in equation 40 is an effective property called the thermal inertia that can be approximated using equation 29 and tabulated values for  $\kappa$ ,  $\rho$ , and  $c$ , (see table A-3) or from the thermal response parameter if  $T_{\text{ign}}$  is measured separately or calculated (see equation 38 and section 4.4). The intercept  $\dot{q}_{\text{loss}}''/\text{TRP}$  of equation 39 can also provide an estimate of  $T_{\text{ign}}$  if an additional expression is introduced to account for the surface heat losses at incipient ignition.

$$\dot{q}_{\text{loss}}'' = \bar{h}(T_{\text{ign}} - T_0) + \varepsilon\sigma(T_{\text{ign}}^4 - T_0^4) \quad (41)$$

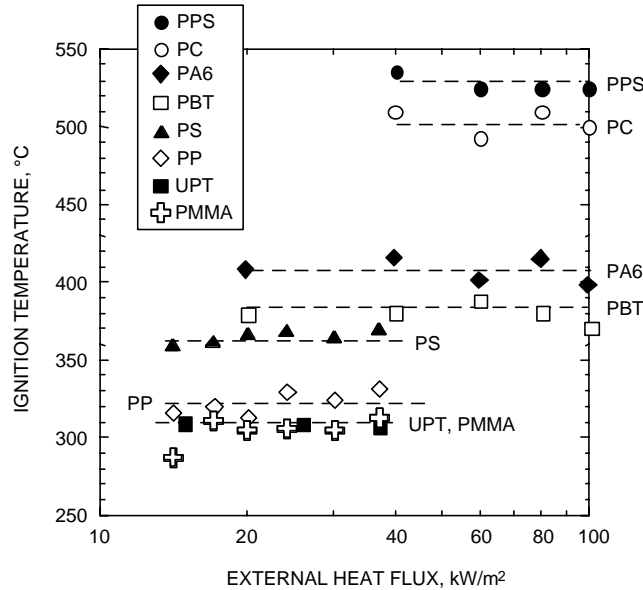


FIGURE 11. IGNITION TEMPERATURE VERSUS EXTERNAL HEAT FLUX FOR PPS, PC, PA6, PBT, PS, PP, UPT, AND PMMA

For a thermally thin sample of thickness  $b$  and at low external heat fluxes near the critical value, the ignition time and external heat flux are related.

$$\frac{1}{t_{\text{ign}}} = \frac{\dot{q}_{\text{ext}}'' - \dot{q}_{\text{loss}}''}{\rho bc(T_{\text{ign}} - T_0)} \quad (42)$$

Equations 39 and 42 state that  $t_{\text{ign}} \rightarrow \infty$  as  $\dot{q}_{\text{ext}}'' \rightarrow \dot{q}_{\text{loss}}''$  at the flash point. In other words, the minimum (critical) value of the external heat flux that can cause ignition is

$$\text{CHF} = \dot{q}_{\text{loss}}''(\text{ignition}) = \bar{h}(T_{\text{ign}} - T_0) + \varepsilon\sigma(T_{\text{ign}}^4 - T_0^4) \quad (43)$$

At the fire point, flaming combustion is first established. If a flame covers a polymer surface having  $\varepsilon \approx 1$  and heat losses are by reradiation only from a surface for which the burning and ignition temperatures are the same, then the first term on the right-hand side of equation 43 is zero, and the critical heat flux (CHF) for burning is

$$\text{CHF}_b = \dot{q}_{\text{loss}}''(\text{burning}) \approx \dot{q}_{\text{rerad}}'' = \sigma T_{\text{ign}}^4 \quad (44)$$

Equations 43 and 44 explain why thermally stable and heat-resistant polymers with high thermal decomposition, ignition, and burning temperatures require a higher heat flux to ignite and burn. Figure 12 shows a plot of the critical heat flux versus the ignition temperature of common polymers measured separately. The solid line is calculated from the abscissa using equation 43 and the dotted line using equation 44.

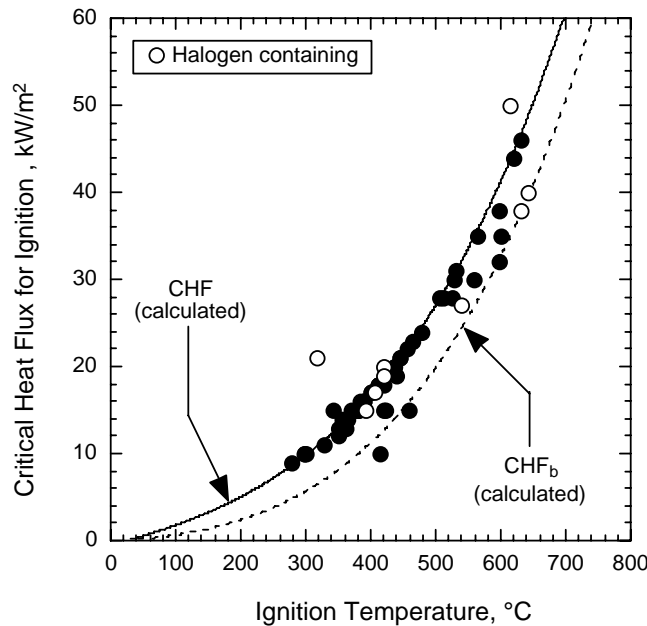


FIGURE 12. CRITICAL HEAT FLUX VERSUS IGNITION TEMPERATURE

### 3.2 STEADY BURNING.

Once ignition is sustained and the burning rate reaches a constant value, the HRR ( $\text{W}/\text{m}^2$ ) of the polymer in steady-flaming combustion is [4, 11, 12, 20, and 21]

$$\text{HRR} = \chi h_c^0 m'' = \chi \frac{h_c^0}{L_g} \dot{q}_{\text{net}}'' \quad (45)$$

where  $\chi$  is the combustion efficiency in the flame and

$$\dot{q}''_{\text{net}} = \dot{q}''_{\text{ext}} + \dot{q}''_{\text{flame}} - \dot{q}''_{\text{loss}} \quad (46)$$

is the net heat flux for steady-flaming combustion with  $\dot{q}''_{\text{flame}}$  the total convective and radiative heat flux from the flame to the polymer surface (see figure 2). The dimensionless ratio of the HOC to the heat of gasification in equation 45 is the heat release parameter (HRP).

$$\chi \frac{h_c^0}{L_g} = \chi(1-\mu) \frac{h_c^0}{h_g} = \text{HRP} \quad (47)$$

Fire calorimetry [4, 11, 20, and 25] (section 5.6) is used to obtain HRP as the slope of HRR versus external heat flux, or as the ratio  $\chi h_c^0/L_g = \text{HOC}/L_g$ , from individual measurements. Table A-5 in appendix A contains HOC and  $\chi$  ( $\equiv \text{HOC}/h_c^0$ ) for common polymers while the HRRs are listed in table A-6. The HOC of the fuel gases,  $h_c^0$ , was measured separately in a pyrolysis-combustion flow calorimeter [26] (section 5.5.2).

Figure 13 shows representative HRR histories for thermally thick and thin samples of polymers that gasify completely or form a char during burning. It is apparent that none of these HRR histories show a constant (steady-state) value of HRR over the burning interval as presumed in equation 45. Consequently, an average HRR for the entire test or over some time interval is typically used in place of a steady HRR. In fact, the interpretation of time varying HRR histories is a subject of active research in fire science. The curves on the left-hand side of figure 13 are characteristic of noncharring ( $\mu = 0$ ) plastics of different thickness. The heat release histories for the charring plastics on the right-hand side of figure 13 show the typical peak in HRR soon after ignition followed by a depression in the HRR as the char layer forms and increases in thickness. The growing char layer insulates the underlying plastic from the surface heat flux so that the net heat flux at the in-depth pyrolysis front decreases with time. Char can also act as a mass diffusion barrier to the volatile fuel. Charring polymers can be linear, branched, or cross-linked thermoplastics, elastomers, or thermosets having amorphous or semicrystalline morphologies.

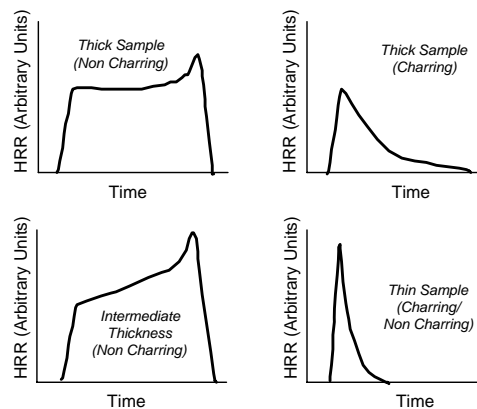


FIGURE 13. REPRESENTATIVE HRR HISTORIES IN FLAMING COMBUSTION FOR THICK AND THIN SAMPLES OF CHARRING AND NONCHARRING POLYMERS

In all cases in figure 13, the time integral (area under the curve) the HRR history per unit mass of polymer consumed by burning is the effective heat of flaming combustion HOC (J/kg). The effective HOC is determined primarily by the fuel chemistry, ventilation rate, and combustion efficiency in the flame. Combustion efficiency is low when halogens are present in the polymer molecule or added as flame-retardant chemicals, when soot or smoke is produced in large yield, or when there is insufficient oxygen for complete conversion of the organic fuel to carbon dioxide and water. Flaming combustion efficiency appears to be relatively independent of the charring tendency of a polymer (compare tables A-2 and A-4 in appendix A).

Figure 14 shows fire calorimetry data for the average HRR of plastics versus their char yield after burning or pyrolysis. The nonlinear dependence of HRR on char yield in figure 14 indicates that charring suppresses the HRR more than can be accounted for by the fuel fraction alone (e.g., equation 47). In fact, charring correlates with thermal stability ( $L_g$ ) and acts as a barrier to the transfer of mass and heat during burning, as illustrated in figure 13, all of which tend to reduce HRR.

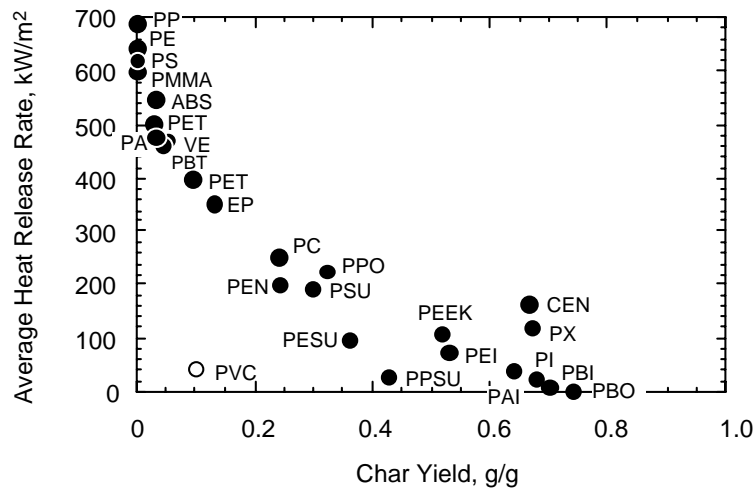


FIGURE 14. AVERAGE HRR IN FLAMING COMBUSTION VERSUS CHAR YIELD OF POLYMERS

### 3.3 UNSTEADY BURNING.

Unsteady burning or transient ignition is the fire behavior that is most relevant to flammability tests [5, 25, and 27]. In flammability tests of flame resistance, a thin strip of polymer is typically subjected to a Bunsen burner flame for several seconds to force ignition, after which the sample is removed from the flame and the duration, extent, and characteristics of burning are recorded. Polymers that continue to burn after removal from the ignition source are considered relatively flammable, while polymers that self-extinguish are relatively flame resistant. Flame resistance is related to fire behavior by combining equations 45-47 and separating the HRR into unforced ( $HRR_0$ ) and forced ( $HRP \dot{q}_{ext}''$ ) components

$$HRR = HRR_0 + HRP \dot{q}_{ext}'' \quad (48)$$

where the HRR in unforced flaming combustion, i.e., in the absence of an external heat flux, is

$$HRR_0 = HRP(\dot{q}''_{\text{flame}} - \dot{q}''_{\text{loss}}) \quad (49)$$

Equation 49 states that the surface flame must provide all the energy to sustain burning in unforced combustion. However,  $\dot{q}''_{\text{flame}}$  contains convective and radiative components and will depend on the size and orientation of the sample with respect to its flaming surface, while  $\dot{q}''_{\text{loss}}$  depends on sample thickness and heat transfer boundary conditions for unsteady burning. Consequently,  $HRR_0$  is generally apparatus- or test-specific. The fire parameters HRP and  $HRR_0$  for a fire calorimeter (section 5.6) can be determined from the slope and intercept, respectively, of a plot of HRR versus external heat flux in a fire calorimeter, as shown in figure 15 for PA6 data from two different sources [4].

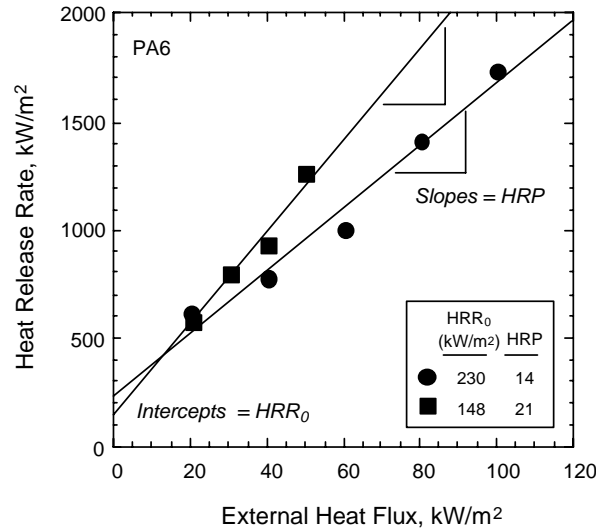


FIGURE 15. HEAT RELEASE RATE VERSUS EXTERNAL HEAT FLUX DATA FOR PA6 FROM DIFFERENT SOURCES

If extinction occurs when the gas phase combustion energy density falls below a minimum (critical) value, analogous to the phenomenon that governs ignition, then equations 38 and 48 provide a criterion for flame extinction in a flammability test. After the sample ignites and the flame is removed  $\dot{q}''_{\text{ext}} = 0$ , the sample will self-extinguish if

$$HRR_0 < HOC \quad \dot{m}''_b = HRR_b^* \quad (50)$$

where  $\dot{m}''_b$  and  $HRR_b^*$  are the critical mass flux and HRR for sustained burning, respectively, in the flammability test (see equations 36-38). From equations 49 and 50, the flame heat flux at the fire point is

$$\dot{q}''_{\text{flame}}(\text{extinction}) \leq \frac{HRR_b^*}{HRP} + \dot{q}''_{\text{loss}} \quad (51)$$

Since  $HRR_b^*$  is test-dependent, the same value that governs horizontal burning and extinction in fire calorimeters ( $HRR_b^* \approx 70 \text{ kW/m}^2$ , see table 2) will not necessarily apply to extinction in an upward flame spread test of a thin strip of polymer. Table A-6 in appendix A lists  $HRR_0$  for common polymers along with their flammability rating in the Underwriters Laboratory vertical or horizontal (UL V, UL H) burning tests for flammability of plastic materials (a Bunsen burner ignition test). Table A-6 shows that when  $HRR_0 < 50 \text{ kW/m}^2$ , as measured in a fire calorimeter, self-extinguishing behavior is observed exclusively in the UL V burning test. Equation 49 shows that  $HRR_0$  decreases as the difference between the heat influx from the flame and the heat efflux by reradiation. Negative  $HRR_0$  values towards the bottom of table A-6 are observed for halogen-containing and flame-retarded plastics that may burn with a low flame heat flux. Negative  $HRR_0$  are also observed for heat-resistant and thermally stable polymers that have high losses and a thermally insulating char. In either case,  $\dot{q}_{\text{flame}}''$  can be less than  $\dot{q}_{\text{loss}}''$  and negative  $HRR_0$  are expected and observed.

Another widely used flammability test is the limiting oxygen index (LOI) [25] test (section 5.5.1). The LOI is a downward-burning test of a thin (3- by 6- by 150-mm) polymer strip in a flowing gas stream whose oxygen concentration is adjusted until the sample flame is on the verge of extinguishing. The dependent variable in the LOI test is the flame heat flux, which increases in rough proportion to the oxygen concentration in the combustion atmosphere (independent variable). The concentration of oxygen in the combustion atmosphere at incipient burning and extinction is the LOI, and this corresponds to a flame heat flux in equation 51.

$$\text{LOI} \propto \dot{q}_{\text{flame}}''(\text{extinction}) = \frac{HRR_b^*}{HRP} + \dot{q}_{\text{loss}}'' \quad (52)$$

A value  $HRR_b^* \approx 100 \text{ kW/m}^2$  has been observed for the LOI test. This value is somewhat higher than the critical HRR for incipient burning and extinction of horizontal slabs ( $HRR_b^* \approx 70 \text{ kW/m}^2$ , see table 2) and upward burning of vertical strips ( $HRR_b^* \approx 50 \text{ kW/m}^2$ ) because heat transfer from the flame is less efficient in downward burning; thus, a higher HRR is necessary for sustained ignition in the LOI test.

The equations for ignition, steady burning, and unsteady burning show that flammability tests measure the fire behavior of the polymer in unforced burning, whether as an after-flame time in a Bunsen burner test (section 5.4) or as an oxygen concentration at incipient extinction (section 5.5). Substituting equations 44 and 38 into equation 51 or 52 gives the efficiency of heat transfer from the flame to the polymer surface in terms of the fire parameter HRP.

$$\frac{\dot{q}_{\text{flame}}''(\text{extinction})}{HRR_b^*} = \frac{HRP}{1 + \frac{\lambda}{HRP}} \quad (53)$$

where  $\lambda = (\sigma/HRR_b^*)(\chi h_c^0 T_0/c_0)^2$  is a dimensionless quantity that is test-dependent by virtue of  $\chi$  and  $HRR_b^*$ . Appendix A table A-6 shows that self-extinguishing behavior in the UL 94 V test and an LOI above 30 is observed exclusively for  $HRP \leq 5$  in these tests where  $HRR_b^* = 75 \pm 25 \text{ kW/m}^2$ . Substituting  $HRP = 4.5 \pm 0.5$  into equation 53 for typical  $\lambda = 20 \pm 5$  (see tables A-2, A-3,

and A-5) gives  $\dot{q}_{\text{flame}}''/\text{HRR}_b^* \approx 0.8$  at incipient extinction in tests of flame resistance. Thus, at incipient extinction and burning, when the combustion zone of the flame is in close proximity to the sample surface, a large fraction ( $\approx 80\%$ ) of the heat released by combustion is used to sustain the burning process.

#### 4. CHEMICAL STRUCTURE AND FIRE PROPERTIES.

A powerful tool to study the effect of chemical structure on the properties of polymers is the additivity principle. The additivity principle, pioneered by Van Krevelen [22], assumes that polymer properties, when expressed per mole of substance, can be calculated by summation of atomic, chemical group, or bond contributions:

$$\mathbf{P} = \sum_j n_i P_i$$

where  $\mathbf{P}$  is a molar property,  $n_i$  is the number of moles of component  $i$  in the polymer repeat unit contributing to the property, and  $P_i$  is the numerical value of the contribution. In the study of fire behavior, the use of specific (mass-based) properties,  $p$ , is more convenient and are related to the molar properties and molecular weight  $M$  of the repeat unit

$$p = \frac{\mathbf{P}}{M} = \frac{\sum_j n_i P_i}{\sum_j n_i M_i}$$

where  $M_i$  is the molar mass of component  $i$ . Additive molar contributions to polymer fire properties  $\kappa$ ,  $\rho$ ,  $c$ ,  $h_{c,p}^0$ ,  $T_p$ , and  $\mu$  are well documented, and their calculation from molar group contributions is straightforward. However, it is often the case that the molar group contributions are not available in the literature for new polymers with novel backbone and pendant structures. Recognizing this limitation of Van Krevelen's group contribution method, Bicerano [28] generalized the additive scheme using graph theory to develop atomic connectivity indices, which replaced the larger chemical groups in the traditional additive approach as the principle descriptors of the topology of the polymer repeat unit. Bicerano's approach is still empirical in that the connectivity indices must be determined from experimental data or by correlation with known group contributions. However, once the connectivity indices are determined for a particular property, that property may be predicted for any chemical structure for which the atomic (as opposed to group) composition is known. The connectivity index method of predicting polymer properties from atomic composition can be accomplished with a hand calculator but is more typically implemented using a stand-alone computer code or accessed as a module in molecular modeling software. Reactive molecular dynamics (RMD) simulations of thermal degradation is a semiempirical method that has recently been applied to the calculation of fuel species and fuel generation rates of polymers [10]. RMD simulations are the most fundamental and powerful approach to understanding and predicting polymer flammability because, unlike the additive approaches, RMD has the potential to predict the products and rates of thermal decomposition, i.e., the fuel generation chemistry.

## 4.1 HEAT TRANSPORT.

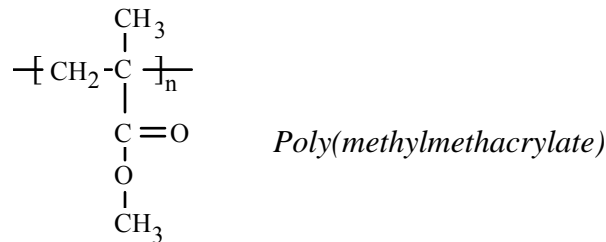
There are no good fundamental theories to predict the thermal conductivity  $\kappa$  (W/m-K), heat capacity  $c$  (kJ/kg-K), or density  $\rho$  (kg/m<sup>3</sup>) of condensed phases (e.g., solid or molten polymers) from chemical structure, but an empirical structure-property correlation allows calculation of these properties from additive atomic or chemical group contributions if the chemical structure of the polymer is known. Table A-3 in appendix A lists the thermal properties of polymers, some of which were calculated from the chemical structure using additive contributions [22 and 28] when experimental values were not available.

## 4.2 HEAT OF COMBUSTION.

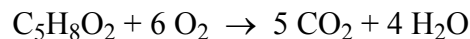
Thermodynamics allow calculation of the heat of combustion,  $h_c^0$ , as the difference between the free energy of the products and reactants in equation 4. Additive molar contributions to the free energy of gaseous, liquid, and solid fuels have been tabulated and used successfully to estimate HOC. A simpler method for calculating or measuring combustion heat is based on the observation that the net heat of complete combustion of organic fuels per mole of oxygen consumed is independent of the chemical composition of the fuel [20]

$$C = h_c^0 \left[ \frac{nM}{n_{O_2} M_{O_2}} \right] = \frac{h_c^0}{r_0} = 13.1 \pm 0.7 \text{ kJ/g} - O_2 \quad (54)$$

where  $h_c^0$  is the net heat of complete combustion of the fuel with all products in their gaseous state,  $n$  and  $M$  are the number of moles and molecular weight of the molecule or polymer repeat unit, respectively,  $n_{O_2}$  is the number of moles of  $O_2$  consumed in the balanced thermochemical equation, and  $r_0$  is the stoichiometric oxygen-to-fuel mass ratio. To illustrate the thermochemical calculation of the net heat of combustion, consider PMMA, which thermally degrades by end-chain scission, unzipping, or depolymerization to monomer in quantitative yield. PMMA has the chemical structure



The methylmethacrylate (MMA) repeat unit in brackets is the volatile fuel species when PMMA burns and has the atomic composition  $C_5H_8O_2$ ; therefore, the balanced chemical equation for complete combustion of PMMA is





Thus, six moles of O<sub>2</sub> are required to completely convert one mole of PMMA repeat unit to carbon dioxide and water. Inverting equation 54, the HOC of the MMA fuel is

$$h_c^0 = C \left[ \frac{n_{O_2} M_{O_2}}{nM} \right] = \frac{(13.1 \text{ kJ/g} - O_2)(6 \text{ mole } O_2)(32 \text{ g } O_2/\text{mole})}{(1 \text{ mole MMA})(100 \text{ g MMA}/\text{mole})} = 25.15 \text{ kJ/g} \quad (55)$$

Net heats of complete combustion of polymers are available in the literature. If the mass fraction of char that remains after burning is  $\mu$ , the fuel fraction is  $(1-\mu)$ , and the heat of complete combustion of the fuel gases,  $h_c^0$ , is related to the HOC of the char,  $h_{c,\mu}^0$ , and polymer,  $h_{c,p}^0$ ,

$$h_c^0 = \frac{h_{c,p}^0 - \mu h_{c,\mu}^0}{1 - \mu} \quad (56)$$

Experimental values for  $h_c^0$  determined by pyrolysis-combustion flow calorimetry (section 5.5.2) are listed in appendix A table A-5. The elemental analysis of chars gives the typical chemical formula C<sub>5</sub>H<sub>2</sub> from which the HOC of the char calculated from oxygen consumption is  $h_{c,\mu}^0 \approx 37 \text{ kJ/g}$ , which can be used to estimate the HOC of the fuel gases of charring polymers using equation 56 if  $\mu$  is known.

### 4.3 ENTHALPY OF GASIFICATION.

In principle, the enthalpy of gasification,  $L_g$ , could be estimated from chemical structure using additive molar contributions or estimated from equation 25 if  $\mu$  is known and  $h_g$  is taken to be 2 MJ/kg. Also relevant to the energetics of fuel generation is the observation that the activation energy for pyrolysis  $E_a$  (J/mole) -measured laboratory TGAs approximates the molar enthalpy of gasification, if  $M_g$  is the molecular weight of the fuel gases [10]

$$L_g = \frac{E_a}{M_g} \quad (57)$$

If  $M$  is the molar mass of the polymer repeat unit, it follows from equation 57 that the ratio

$$\frac{M_g}{M} = \frac{E_a}{ML_g} \quad (58)$$

should be characteristic of the mode of thermal degradation. For example, polymers, such as PMMA, polyoxymethylene (POM), and to a first approximation, PS, that thermally degrade by end-chain scission (depolymerize or unzip) produce monomer at near-quantitative yield. Consequently, these polymers should have  $M_g \approx M$  or  $M_g/M \approx 1$ . Polymers such as PE and PP that decompose by main-chain scission (cracking) to multimonomer fragments will have  $M_g/M > 1$ . Conversely, polymers with complex molecular structures and high molar mass repeat units ( $M \geq 200 \text{ g/mole}$ ), such as polyamides (PA), cellulose, polyethyleneterephthalate (PET), or PC, that degrade by random scission, cyclization, small molecule splitting, or by chain-stripping

of pendant groups such as polyvinylchloride (PVC) yield primarily low molar mass species (water, carbon dioxide, alkanes, and mineral acids) relative to the repeat unit so that for these materials  $M_g/M < 1$ . Table 3 shows fuel and monomer molar mass ratios,  $M_g/M$ , calculated as  $E_a/ML_g$ , according to equation 58, for some of the polymers in table A-2. Global pyrolysis activation energies for the thermally stable engineering plastics listed in the last four rows of table 3 are estimated to be in the range  $E_a = 275 \pm 25$  kJ/mole. Qualitative agreement is observed between the modes of pyrolysis (end-chain scission, random scission, and chain-stripping) and the calculated fragment molecular weight using equation 58, suggesting that the global pyrolysis activation energy determined from thermogravimetry experiments approximates the molar enthalpy of pyrolysis of the degradation products.

TABLE 3. HEATS OF GASIFICATION, PYROLYSIS ACTIVATION ENERGY, CHAR YIELD, AS WELL AS CALCULATED AND MEASURED MOLECULAR WEIGHTS OF DECOMPOSITION PRODUCTS FOR SOME POLYMERS

Polymer	M (g/mol)	$L_g$ (kJ/g)	$\mu$ (g/g)	$h_g$ (kJ/g)	$E_a$ (kJ/mol)	$M_g/M$	Pyrolysis Products
Chain Cracking							
PP	42	1.9	0	1.9	243	3.0	C <sub>2</sub> -C <sub>90</sub> saturated and unsaturated hydrocarbons
PE	28	2.2	0	2.2	264	4.3	
Unzipping							
PS	104	1.8	0	1.8	230	1.2	40%-60% monomer
PMMA	100	1.7	0	1.7	160	0.94	100% monomer
POM	30	2.4	0	2.4	84	1.2	100% monomer
Intramolecular Scission							
PA 66	226	2.1	0	2.1	160	0.3	H <sub>2</sub> O , CO <sub>2</sub> , C <sub>5</sub> HC's
PVC	62	2.7	0.1	2.4	110	0.7	HCl, benzene, toluene
Cellulose	162	3.2	0.2	2.6	200	0.5	H <sub>2</sub> O , CO <sub>2</sub> , CO
PT	131	5.0	0.6	2.0	178	0.3	Complex mixture of low molecular weight products
PC	254	2.4	0.3	1.7	200	< 1	
PEI	592	3.5	0.5	1.8	≈ 275	< 1	
PPS	108	3.8	0.5	1.9	≈ 275	< 1	
PEEK	288	3.4	0.5	1.7	≈ 275	< 1	
PAI	356	4.8	0.6	1.9	≈ 275	< 1	
PX	180	6.4	0.7	1.9	≈ 275	< 1	

#### 4.4 IGNITION TEMPERATURE.

Common sense and much experimental data suggest that the ignition temperature and thermal decomposition temperature of polymers should be related since mass loss and fuel generation begins in earnest at these temperatures. However, the heating rate in a fire is on the order of 10-20 times higher than the heating rates normally used to measure thermal decomposition temperatures in laboratory thermogravimetry experiments. Figure 11 and equation 38 show that

the ignition temperature of polymers is not particularly sensitive to heat flux (heating rate), while equation 23 states that the thermal decomposition temperature of polymers in TGA experiments increases by about 45°C for each 10 fold increase in heating rate. Consequently, there should be a heating rate  $\beta_{\text{ign}}$  in a TGA experiment for which the ignition and decomposition temperatures of polymers are equal, i.e.,  $T_{\text{ign}} = T_p(\beta_{\text{ign}})$ . Substituting equation 57 into equation 38

$$T_{\text{ign}} = \left[ \frac{T_0 L_g}{c_0} \right]^{\frac{1}{2}} = \left[ \frac{T_0 E_a}{M_g c_0} \right]^{\frac{1}{2}} \quad (59)$$

Setting this result equal to  $T_p$  in equation 23

$$\left[ \frac{T_0 E_a}{c_0 M_g} \right]^{\frac{1}{2}} = \frac{E_a}{R \ln(\beta^*/\beta_{\text{ign}})} \quad (60)$$

Equation 60 can be evaluated at  $T_0 = 293$  K using the properties in table 4, with the result that the heating rate for which  $T_{\text{ign}} = T_p(\beta_{\text{ign}})$  is of the order

$$\beta_{\text{ign}} = \beta^* \exp \left[ -\frac{E_a c_0 M_g}{R^2 T_0} \right]^{\frac{1}{2}} \approx 1\text{-}3 \text{ K/min} \quad (61)$$

which is at the lower range of heating rates typically used in nonisothermal TGA experiments,  $\beta = 10\text{-}20$  K/min. From equations 59-61, the ignition and decomposition temperatures are related.

$$\frac{1}{T_{\text{ign}}} = \frac{1}{T_p} + \frac{R \ln(\beta/\beta_{\text{ign}})}{E_a}$$

TABLE 4. THERMOKINETIC PROPERTIES OF PMMA, PE, AND PHENOLIC TRIAZINE

Polymer	$\ln[\beta^*, \text{K/s}]$	$c_0$ (kJ/kg-K)	$E_a$ (kJ/mole)	$M_g$ (kg/mole)
PMMA	30	1.4	160	0.10
PE	43	1.5	264	0.11
Phenolic Triazine	36	1.5	178	0.12

Consequently,  $T_p$  measured in a TGA in an inert environment at heating rates  $\beta/\beta_{\text{ign}} \approx 10$  can be 25-50 K higher than the ignition temperature (see table A-1) for typical  $E_a \approx 200$  kJ/mole. Figure 16 shows a plot of the data in table A-1 for the measured ignition temperature of polymers versus their mean thermal decomposition temperature  $(T_d + T_p)/2$ . The use of a mean thermal decomposition temperature rather than  $T_p$  as an estimate of  $T_{\text{ign}}$  compensates for most of the heating rate effects described by equations 59-61. Also contained in figure 16 are data for

the incipient burning (fire point) and incipient ignition (flash point) temperatures of hydrocarbon oils plotted on the ordinate and abscissa, respectively.

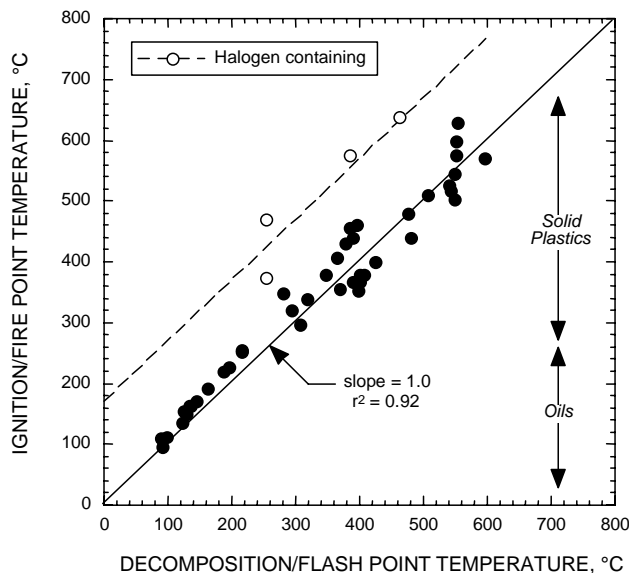


FIGURE 16. IGNITION/FIRE POINT TEMPERATURE VERSUS DECOMPOSITION/FLASH POINT TEMPERATURE FOR SOLID AND LIQUID FUELS

Because of its importance to flammability, Van Krevelen identified a number of experimental indices that can be used to characterize the short-term thermal stability of a polymer [22]. The indices, which are determined from temperature scanning thermogravimetry experiments at constant heating rates of 3-10 K/min are  $T_d$ , the temperature in Kelvin at which the polymer weight loss is just measurable;  $T_{d,1/2}$ , the temperature at which the weight loss reaches 50% of its final value;  $T_{d,max}$ , the temperature at the maximum rate of weight loss; and  $E_a$ , the activation energy for pyrolysis. Noting that all of these temperatures depend on heating rate and that  $T_{d,max}$  is identical to  $T_p$  in the present work, Van Krevelen proposed the following interrelationships based on tabulated data for 37 polymers (all temperatures are Kelvin):

$$T_d = 0.9 T_{d,1/2} \quad (62)$$

$$T_{d,max} = T_p \approx T_{d,1/2} \quad (63)$$

$$T_p \approx 423 + E_a \text{ (kJ/mole)} \quad (64)$$

Equation 64 can be cast in the form of equation 23 by defining a reference temperature  $T_0 = E_a/R \ln(\beta^*/\beta_0) = 423 \text{ K}$ . Equations 62-64 imply that  $T_p$  or  $T_{d,1/2}$  can be used as the primary indicator of thermal stability with the other indices being roughly estimated from it. A plot of  $T_p$  versus  $E_a$  from thermogravimetric analyses of various polymers at heating rates on the order of 10 K/min is shown in figure 17. The trend is in qualitative agreement with equation 64 but the correlation coefficient is too low ( $< 0.5$ ) for predictive purposes. For this reason, Van Krevelen extended the use of additive molar group contributions to the calculation of the thermal decomposition temperature. In Van Krevelen's method of calculating the thermal decomposition temperature,

the molar thermal decomposition function  $Y_{d,1/2}$  is related to the product of the polymer repeat unit molecular weight  $M$  and the decomposition temperature viz.

$$M \cdot T_{d, 1/2} = Y_{d, 1/2} \quad (65)$$

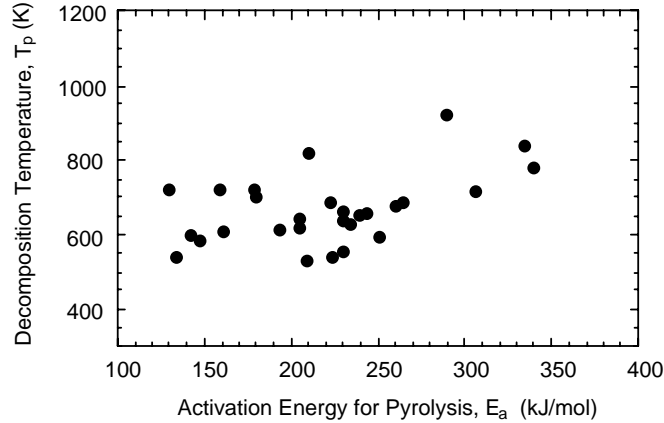
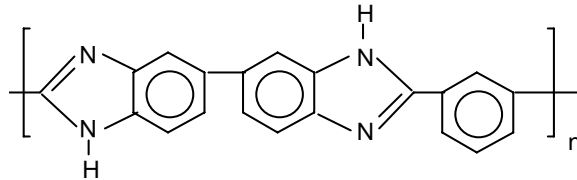


FIGURE 17. PYROLYSIS TEMPERATURE VERSUS ACTIVATION ENERGY OF POLYMERS

The decomposition temperature is calculated by summing the individual molar decomposition functions  $Y_{d, 1/2}^i$  for each chemical group of molar mass  $M_i$  comprising the repeat unit

$$T_{d,1/2} = \frac{Y_{d,1/2}}{M} = \frac{\sum_j n_j Y_{d,1/2}^i}{\sum_j n_j M_i} \quad (66)$$

The molar group contribution  $Y_{d, 1/2}^i$  for each of the chemical groups comprising the polymer were determined for decomposition temperatures measured at a linear heating rate  $\approx 3$  K/min. For example, the decomposition temperature of 2,2'-m-phenylene-5,5'-bibenzimidazole (PBI), having the chemical repeat unit structure

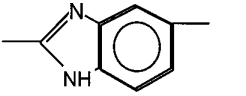
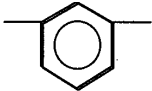


is calculated from the  $Y_{d, 1/2}^i$  in table 5 and equation 66 as

$$T_p = \frac{(2)(105) + (1)(65)}{(2)(116.12) + (1)(76.09)} \times 1000 = 892 \text{ K} = 619^\circ\text{C}$$

which is in general agreement with the literature value  $T_p \approx 903$  K and the data in table A-1 and figure 6.

TABLE 5. GROUP CONTRIBUTIONS TO THE DECOMPOSITION TEMPERATURE OF POLYBENZIMIDAZOLE

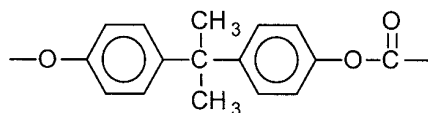
Structural Group, <i>i</i>	$n_i$	$M_i$ (g/mole)	$Y_{d,1/2}^i$ (g-K/mole)
	2	116.12	105
	1	76.09	65

#### 4.5 CHAR YIELD.

Pyrolysis/char residue has the character of a thermodynamic quantity since it depends only on temperature and the composition of the material through the enthalpy barriers to gas and char formation,  $E_g$ , and  $E_c$ , in equation 19. The char-forming tendency of different groups is additive and roughly proportional to the aromatic (i.e., nonhydrogen) character of the group (see figure 9). The char yield is calculated by summing the char-forming tendency per mole of carbon of the chemical groups  $C_{FT,i}$  and dividing by the molecular weight of the repeat unit [22].

$$Y_c = \frac{C_{FT}}{M} \times M_{\text{carbon}} = \frac{\sum_j n_j C_{FT,j}}{\sum_j n_j M_j} \times 12 \quad (67)$$

The  $C_{FT,i}$  are the moles carbon remaining as char per mole of chemical group  $i$  in the polymer measured at 850°C. Negative corrections are made for aliphatic groups containing hydrogen atoms in proximity to char-forming groups because of the possibility for disproportionation and subsequent volatilization of hydrogen-terminated chain fragments that are no longer capable of recombining and cross-linking to make char. Table 6 lists the char-forming tendency of the structural units comprising bisphenol-A polycarbonate whose chemical structure is


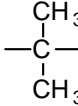
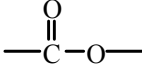
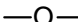


From the data in table 6 and equation 67, the char yield of polycarbonate is calculated to be

$$Y_c = \frac{(2)(4) + (1)(-3) + (1)(0) + (1)(0)}{(2)(76) + (1)(42) + (1)(16) + (1)(44)} \times 12 = 0.24 = 24\%$$

which compares with the measured value  $Y_c = 0.25$  in appendix A, table A-2. The method is empirical and relatively simple to use, and good agreement is obtained with other measured pyrolysis residues in table A-2. The char yield of polymers under anaerobic conditions is well described using the additive molar contributions of the individual structural groups comprising the polymer.

TABLE 6. GROUP CONTRIBUTIONS TO THE CHAR YIELD OF BISPHENOL-A POLYCARBONATE

Structural Group, i	$n_i$	$M_i$ (g/mole)	$C_{FT,i}$ (mole-C/mole)
	2	76.10	4
	1	42.08	-3
	1	44.01	0
	1	16.00	0

#### 4.6 HEAT RELEASE RATE.

Individually, the material and combustion properties  $\kappa$ ,  $\rho$ ,  $c$ ,  $h_{c,p}^0$ ,  $T_p$ , and  $\mu$  have found limited success as descriptors of fire behavior because the coupling of gas and condensed phase burning processes are complex (e.g., figure 2). Direct measurement of fire behavior or flammability requires about one kilogram of material from which to prepare samples and is, therefore, prohibitively expensive for research where only gram quantities are typically available. Separate determination of thermochemical and combustion properties using laboratory thermal analyses and combustion calorimetry requires only gram quantities of material, but the process is time consuming. Consequently, recent work has focused on identifying a flammability parameter that captures the chemical dynamics of flaming combustion in a single laboratory test using research (gram) quantities of material [10, 26, and 29].

The HRR in flaming combustion HRR is the amount of heat,  $Q$ , released by gas phase combustion of unit mass of fuel,  $m$ , released by pyrolysis per unit time,  $t$ , and per unit area of burning surface,  $S$ . A simple dimensional analysis gives

$$\text{HRR} = \frac{1}{S} \frac{dQ}{dt} = \rho \delta \left( \frac{1}{m} \frac{dQ}{dt} \right) = \rho \delta \dot{Q}_c \quad (68)$$

where  $\rho$  and  $\delta$  are the average density and thickness of the mesophase, respectively. If a specific HRR is defined, that is, equation 22 multiplied by the HOC of the pyrolysis and fuel gases,  $h_c^0$

$$\dot{Q}_c = \beta \left( \frac{h_c^0 (1 - \mu) E_a}{eRT_p^2} \right) = \beta \eta_c \quad (69)$$

where

$$\eta_c = \frac{h_c^0 (1 - \mu) E_a}{eRT_p^2} \approx \frac{h_{c,p}^0}{\Delta T_p} \quad (70)$$

is a collection of thermal and combustion properties with the units (J/kg-K) and significance of a heat release capacity. The heat release capacity is the maximum amount of heat released by combustion per degree of temperature rise per unit mass of polymer in the mesophase. If the heating rate in the mesophase is  $\beta$ , then  $\eta_c$  is related to HRR.

$$\text{HRR} = \eta_c (\chi\rho\delta\beta) = \eta_c f(\dot{q}_{\text{net}}'') \quad (71)$$

where  $f(\dot{q}_{\text{net}}'') = \chi\rho\delta\beta$  is an increasing function of the external heat flux with units of kg-K/m<sup>2</sup>-s. Figure 18 is a plot of the average HRR at an external heat flux of about  $50 \pm 10 \text{ kW/m}^2$  versus  $\eta_c$  for the same or similar polymers. The proportionality between HRR and  $\eta_c$  in figure 18 is reasonably good considering that the coefficient of proportionality  $f(\dot{q}_{\text{net}}'') = f(\dot{q}_{\text{ext}}'' + \dot{q}_{\text{flame}}'' - \dot{q}_{\text{loss}}'')$  varies with thermal stability, char-forming tendency, mesophase density, and flaming combustion efficiency in a complex way.

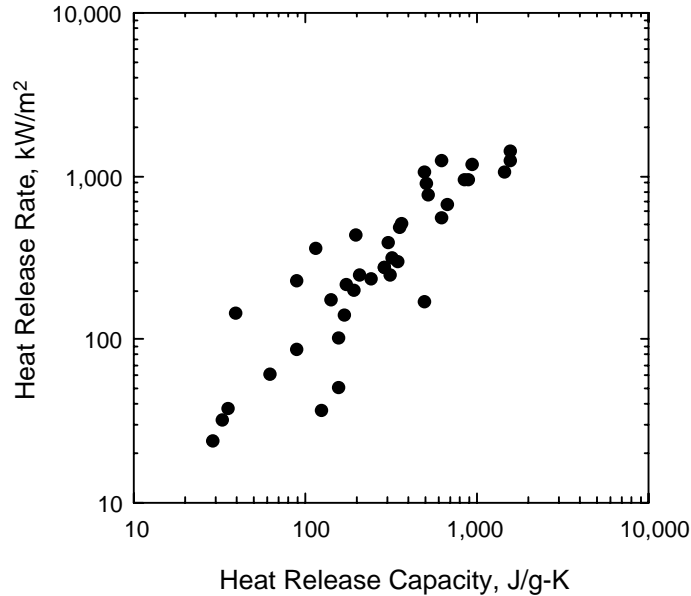


FIGURE 18. AVERAGE HRR VERSUS HEAT RELEASE CAPACITY OF POLYMERS

Equation 70 is an explicit result for a parameter,  $\eta_c$ , that contains most of the properties known to correlate with flammability. In particular,  $\eta_c$  is proportional to the fuel fraction and HOC of the fuel and inversely proportional to thermal stability (heat resistance). Because  $\eta_c$  is a combination of material properties, each of which is calculable from additive molar group contributions,  $\eta_c$  itself should be calculable from the same or similar molar groups if it is a material property.

From the additivity principle for polymer properties, a molar heat release capacity,  $\Psi$ , is defined [29] with units of J/mole-K whose functional form is equation 70 but with the thermal stability and combustion properties written as additive molar quantities,  $\mathbf{H}$ ,  $\mathbf{V}$ ,  $\mathbf{E}$ , and  $\mathbf{Y/M}$  in place of  $h_c^0$ ,  $(1-\mu)$ ,  $E_a$ , and  $T_p$ , respectively. If each chemical group  $i$  in the polymer adds to the component



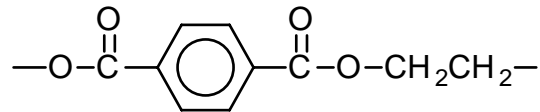
molar properties according to its mole fraction  $n_i$  in the repeat unit, then in terms of molar quantities, equation 70 becomes

$$\Psi = \frac{\mathbf{HVE}}{eR(\mathbf{Y/M})^2} = \frac{\left(\sum_i n_i H_i\right)\left(\sum_i n_i V_i\right)\left(\sum_i n_i E_i\right)}{eR\left(\sum_i n_i Y_i/M_i\right)^2} \quad (72)$$

with  $H_i$ ,  $V_i$ ,  $E_i$ ,  $Y_i$ , and  $M_i$  the molar heat of combustion, mole fraction of fuel, molar activation energy, molar thermal decomposition function, and molar mass of component  $i$ , respectively. Expanding the summations in equation 72 and retaining only the noninteracting terms for which  $i = j = k \dots$  (i.e., neglecting terms containing products and quotients with mixed indices), the heat release capacity on a mass basis is

$$\eta_c = \frac{\Psi}{M} = \frac{\sum_j n_j \Psi_j}{\sum_j n_j M_j} = \frac{\sum_j N_j \Psi_j}{\sum_j N_j M_j} \quad (73)$$

Experimental heat release capacities,  $\eta_c$ , have been measured for over 200 polymers, and the results were used to generate over 30 additive molar group contributions by treating the  $\Psi_i$  as adjustable parameters in equation 73 for polymers with known chemical structures [29]. Table A-6 in appendix A contains  $\eta_c$  for a few dozen polymers. Figure 19 compares calculated and measured heat release capacities for 50 polymers using the 30 empirical  $\Psi_i$ , determined by Walters and Lyon (2003). Overall agreement between measured and calculated values is about 15%, which is encouraging at this early stage of research. Additive contributions to the heat release capacity are being updated as more polymers are tested and the measurement technique improves. As an example of the additive procedure for calculating the heat release capacity, the chemical repeat unit for PET is



for which the most recent chemical group contributions are listed in table 7. Combining the  $N_i$ ,  $M_i$ , and  $\Psi_i$  for PET, per equation 73

$$\eta_c = \frac{\sum N_i \Psi_i}{\sum N_i M_i} = \frac{(1)(28.8) + (2)(0) + (2)(16.7)}{(1)(76.10) + (2)(44.01) + (2)(14.03)} = \frac{62.2 \text{ kJ/mole-K}}{192.18 \text{ g/mole}} = 324 \frac{\text{kJ}}{\text{kg-K}}$$

The predicted heat release capacity for PET compares favorably with typical experimental values for this polymer  $\eta_c = 326 \pm 52 \text{ kJ/kg-K}$  (see table A-6), considering that the group contributions are average values derived from several different polymers.

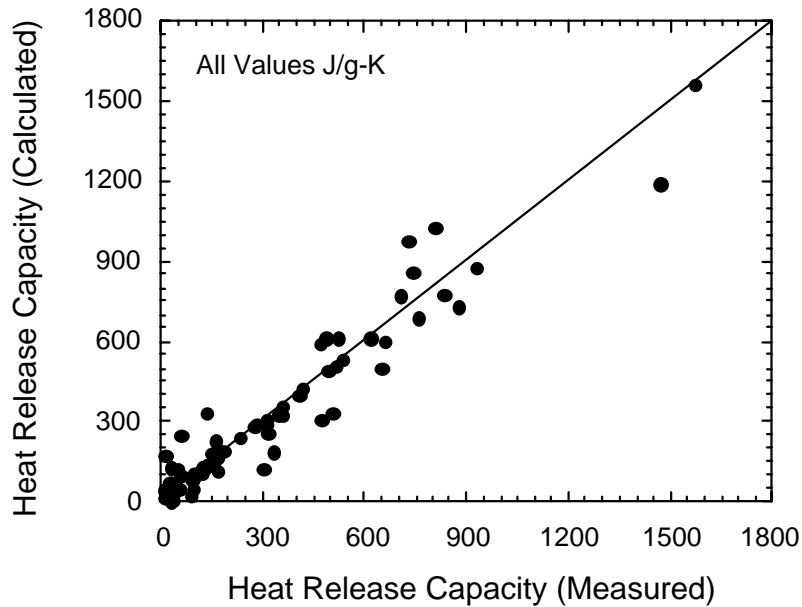

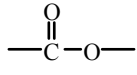
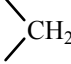


FIGURE 19. POLYMER HEAT RELEASE CAPACITIES: CALCULATED VERSUS MEASURED VALUES

TABLE 7. GROUP CONTRIBUTIONS TO THE HEAT RELEASE CAPACITY OF PET

Structural Group, i	$n_i$	$M_i$ (g/mole)	$\Psi_i$ (kJ/mole-K)
	1	76.10	28.8
	2	44.01	0.0
	2	14.03	16.7

#### 4.7 FLAME RESISTANCE.

Flame resistance is the ability to withstand flame impingement or give protection from it. Equation 53 shows that a critical HRR criterion for incipient burning and extinction gives a simple scaling relationship between flame resistance and fire behavior in terms of the HRP. At the molecular level, HRR is governed by the heat release capacity (section 4.6), which is proportional to HRR in steady burning (equation 71) for a particular set of test conditions and material properties. Heat release capacity can be related to flame resistance in the same way that HRR was related to flame resistance (section 3.3). If the HRR is equation 71 and the criterion for flame extinction in flammability tests is equation 50, then flame extinction is related to heat release capacity.

$$\text{HRR} = \eta_c f(\dot{q}_{\text{flame}}'' - \dot{q}_{\text{loss}}'') \leq \text{HRR}_b^* \quad (74)$$

Equation 74 states that (analogous to HRR) there is a critical value of  $\eta_c$  below which flame extinction will occur in a flammability test.

$$\eta_c \leq \frac{\text{HRR}_b^*}{f(\dot{q}_{\text{flame}}'' - \dot{q}_{\text{loss}}'')} \quad (75)$$

Figure 1 showed generic  $\eta_c$  and flame resistance results for commercial polymers. Figure 20 shows grouped ratings for 50 polymers in the UL V and UL H tests for flammability of plastics [27] (section 5.4 and table 8). Three ranges of flammability are observed with respect to  $\eta_c$  in figures 1 and 20: (1) no ignition in a vertical test (UL 94 V0 rating or better) for  $\eta_c < 200$  kJ/kg-K, (2) self-extinguishing (UL 94 V) behavior after 10-30 seconds of burning in a vertical test for  $\eta_c = 200$ -400 kJ/kg-K, and (3) a self-propagating flame in a horizontal burning test for  $\eta_c > 400$  kJ/kg-K.

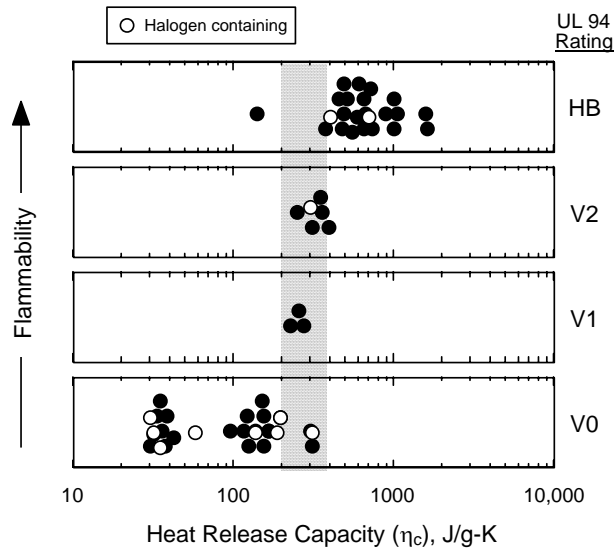


FIGURE 20. FLAMMABILITY RATING IN UL 94 TEST VERSUS HEAT RELEASE CAPACITY OF 50 POLYMERS

TABLE 8. UL 94 20-mm VERTICAL BURNING TEST CLASSIFICATION CRITERIA

Observation	Classification		
	V-0	V-1	V-2
$t_1$ or $t_2$ for any specimen	10 s	30 s	30 s
$t_1 + t_2$ for 5 specimens	50 s	250 s	250 s
$t_2 + t_3$ for any specimen	30 s	60 s	60 s
Afterflame or afterglow up to clamp, any specimen	No	No	No
Ignition of cotton	No	No	Yes

With regard to flammability as measured in the LOI test [25] (section 5.5.1), if equation 52 applies and  $\dot{q}_{\text{flame}}^{\prime\prime}(\text{extinction}) = \phi \text{ LOI}$ , then equation 74 gives the criterion for flame extinction in the LOI test.

$$\eta_c \leq \frac{\text{HRR}_b^*}{f(\phi \text{ LOI} - \dot{q}_{\text{loss}}^{\prime\prime})} \quad (76)$$

Equation 76 suggests that LOI and  $\eta_c$  are inversely related. Figure 21 shows a plot of generic values of LOI versus  $\eta_c$  (see table A-6 in appendix A). A power law,  $\text{LOI} = 125/\eta_c^{1/4}$ , can be fit to the data with reasonable accuracy (correlation coefficient = 0.84), confirming the inverse relationship between LOI and  $\eta_c$  suggested by equation 76.

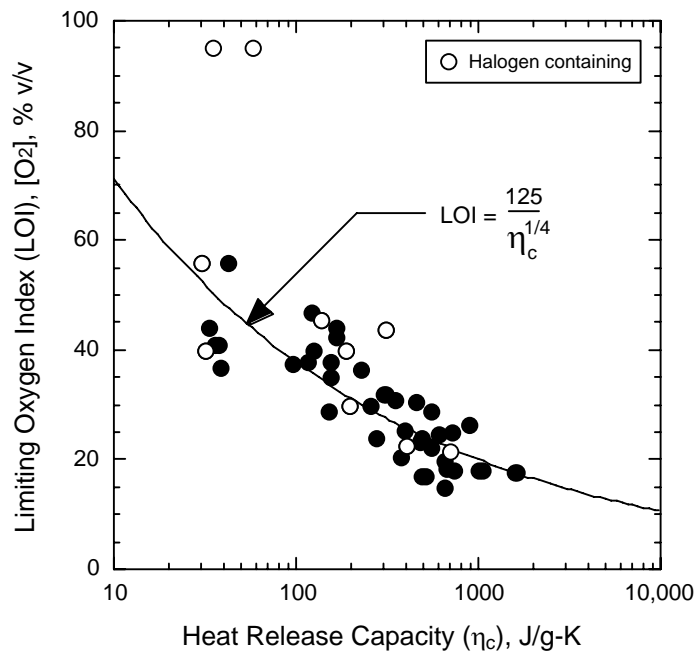


FIGURE 21. LIMITING OXYGEN INDEX VERSUS HEAT RELEASE CAPACITY FOR 50 POLYMERS

#### 4.8 SMOKE.

The smoke extinction area (SEA,  $\text{m}^2/\text{kg}$ ) is a global measure of the condensed phase (liquid and solid) products of flaming combustion, having units of square meters of particulate scattering surface per kilogram of material burned. The SEA is measured in a fire calorimeter under well-ventilated conditions from optical extinction of the combustion gas stream [25]. Appendix A, table A-7 lists the specific SEA for a variety of polymers averaged from the literature. Figure 22 shows a plot of SEA data in table A-7 versus the flaming combustion efficiency of the same polymer listed in table A-5. It is seen that SEA varies by a factor of 100 between different polymers and is particularly sensitive to combustion efficiency in the range  $\chi = 0.8-1.0$ . Below  $\chi = 0.8$ , SEA is essentially independent of combustion efficiency.

The effect of chemical structure on smoke production can generally be described as follows. Aliphatic oxygenated fuels (POM, PMMA, and PA) and those with high thermal stability (PBI, PAI, PEI, PES, PEEK, and Polyarylsulfone) or an extremely low burning rate (polytetrafluoroethylene, chlorinated polyvinylchloride, and wood) tend to produce less smoke per unit mass of material burned than aliphatic (PE and PP), aromatic oxygen- and nitrogen-containing (PET, PBT, epoxy (EP), PC, polyurethane (PU), bismaleimide, VE, and PPO) or aromatic sulfur-containing (PSU and PPS) polymers.

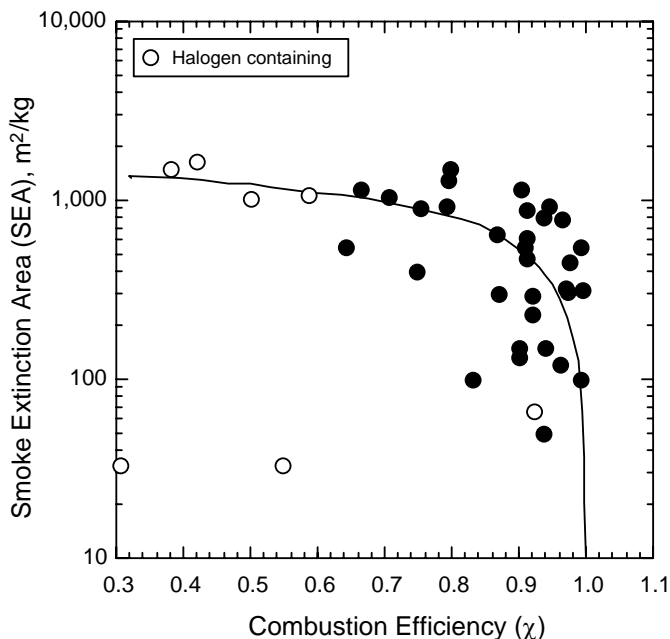


FIGURE 22. SMOKE EXTINCTION AREA VERSUS FLAMING COMBUSTION EFFICIENCY ( $\chi$ ) FOR 40 POLYMERS

Polymers with low thermal stability and pendant (acrylonitrile-butadiene-styrene terpolymer (ABS) and PS) or backbone (EP, unsaturated polyester thermoset (UPT), VE, and PPO) aromatic groups produce a large amount of smoke because their thermal degradation products (fuel gases) contain the aromatic nucleus for soot formation (see section 2.1).

Low thermal stability aromatic polymers with high SEA (ABS, EP, and PS) produce 50% more smoke per unit mass when brominated flame-retardants are added to inhibit combustion. These materials, listed at the bottom of table A-7 in appendix A, produce 5-20 times more smoke per unit mass than the commodity and engineering polymers in the top half of the table. Silicones are anomalous with respect to SEA because the scattering particles are silica ( $SiO_2$ ), which is a complete (rather than incomplete) combustion product of the backbone silicon.

The highest SEAs are associated with halogen-containing polymers (rigid and flexible PVC and PMMA/PVC alloy) apparently because of combustion inhibition by chlorine (see equations 1-3 and figure 22).

The smoke point is another measure of the tendency of a fuel to produce smoke and this quantity, like smoke extinction area, is related to the chemical composition and structure of the fuel. The smoke point is defined as the minimum fuel mass flow rate at which smoke first escapes from the tip of a laminar diffusion flame (see figure 2), i.e., the residence time of the smoke in the combustion zone becomes too short to effect complete oxidation. The results of the smoke point test are qualitatively similar to the SEA data in table A-7 with respect to chemical structure and smoke-forming tendency. In particular, it was found that the smoke-forming tendency, as determined by smoke point measurements, was lowest for oxygenated fuels (alcohols, aldehydes, esters, and ethers) and increases through the series—alkanes, branched alkanes, alkenes, and aromatics.

## 5. FIRE AND FLAMMABILITY TESTS.

### 5.1 TERMINOLOGY: FIRE VERSUS FLAMMABILITY.

There is no universal agreement on the definition of flammability tests and how they are different from fire tests. A common application of fire and flammability tests is to obtain data for regulatory compliance, as will be discussed in the next section. Fire safety codes and regulations are generally based on two strategies. The first strategy involves preventing or, at least, minimizing the likelihood of ignition. Since, in practice, it is not possible to completely eliminate ignition, the second strategy involves managing the impact of a subsequent fire.

Flammability tests are typically associated with the first strategy. A small specimen (linear dimensions of the order of centimeters or inches) of a polymer is exposed to a small heat source (Bunsen burner type flame, hot wire, etc.) for a short duration (seconds). Pass/fail criteria are based on ignition of the specimen during exposure, formation of flaming droplets or sustained flaming or smoldering after removal of the heat source.

For the purpose of this report, fire tests are associated with the second strategy and defined as experimental methods to characterize the behavior of polymers under more severe thermal exposure conditions that are representative of the growth phase of a cargo compartment fire. These conditions are simulated with a gas-fired or electrical heater or a large gas burner turbulent diffusion flame (flame length of the order of a meter or several feet). The incident heat flux to the specimen is primarily radiative when heaters are used and mainly convective for flame exposure. Total incident heat flux varies from approximately 1 kW/m<sup>2</sup> to more than 100 kW/m<sup>2</sup>. Note that the maximum radiant heat flux from the sun on earth is approximately 1 kW/m<sup>2</sup>. Polymers that are not treated with fire-retardant chemicals typically ignite when exposed to heat fluxes of 10-20 kW/m<sup>2</sup> in the presence of a small pilot flame or hot spark.

The aforementioned definitions imply that flammability tests are concerned with a lower level of performance. Passing a flammability tests does not mean that a material will be less hazardous when involved in a fire. This is consistent with one definition of the term flammable, which is described in ASTM E 176, “Terminology of Fire Standards,” as “subject to easy ignition and rapid flaming combustion” [25].

The characteristics that are measured in a fire test are indicative of the performance of the material under the conditions of the test and are, therefore, referred to as fire-test-response

characteristics. They may or may not be indicative of the hazard of a material under actual fire conditions. The most common fire-test-response characteristics that are measured in fire tests are the ease of ignition, flame spread, heat release, smoke generation, and toxic potency of smoke [20 and 25].

## 5.2 FIRE AND FLAMMABILITY TEST APPLICATIONS.

There are three distinct applications of fire and flammability tests, which are discussed below.

### 5.2.1 Regulatory Compliance.

Codes and regulations have been developed in many countries to ensure a level of public fire safety that is acceptable to society. The main objectives of these codes and regulations in terms of fire and flammability of materials are to limit the likelihood of ignition and to reduce the rate of fire growth to the critical stage of flashover in the compartment of fire origin. In addition, codes and regulations also limit the quantities of particulate matter (affects visibility) and of toxic and corrosive products of combustion that can cause human casualties and excessive damage to equipment.

Codes and regulations are intended to provide a minimum level of safety based on loss objectives that are acceptable to society. Other stakeholders often specify additional requirements. For example, an insurance company might have more stringent requirements to reduce the risk of incurring excessive losses in the event of a fire. Building owners and operators might require a level of safety that exceeds the building code. Manufacturers of transportation vehicles might issue specifications for their product suppliers that go beyond the regulations.

Codes, regulations, and specifications specify acceptance criteria for the products that are used in specific areas of the environment that is regulated. These criteria are based on performance in one or more fire or flammability tests. This approach has been applied extensively to two environments where the potential exists for large life loss: buildings and transportation vehicles. Some important fire and flammability tests that are used in different parts of the world to ensure a specific level of safety in these two environments are summarized in the following sections.

### 5.2.2 Quality Assurance and Research.

Fire and flammability tests are also used in support of production control. The objective of a production control program is to ensure that a product which is sold in the marketplace is identical to the specimen that was originally tested for regulatory compliance. Often, it is not practical or economically feasible to use the qualification test(s) in a follow-up production control program, and a simple test is often adequate to verify the consistency of the product. Relatively simple flammability tests are, therefore, most often used for the purpose of quality assurance. The same tests are then used in research and development of new products.

### 5.2.3 Data for Fire Safety Engineering Design and Analysis.

Fire safety codes and regulations are largely prescriptive. This means that they contain acceptance criteria for materials, products, and assemblies based on performance in one or

several tests. The overall level of safety that is accomplished is not explicitly stated. Sometimes it is not possible to demonstrate that a material, product, or assembly meets the specified acceptance criteria. For example, it might not be possible to obtain a valid test result for a product that melts and shrinks away from the heat source in a fire test. Fire safety codes and regulations generally contain a clause that gives the enforcing official the authority to accept a variance from the specified acceptance criteria. To persuade the enforcing official, it is necessary to demonstrate that the material, product, or assembly does not compromise the level of safety that is implicit in the code or regulation. This usually requires an engineering analysis and tests to obtain material properties that are needed in support of the analysis.

In recent years, performance-based codes and regulations have become increasingly popular. Such codes and regulations explicitly state the minimum level of performance of the system (building, railcar, etc.) in case of fire. That a particular design meets the specified level of performance is again based on an engineering analysis. Similar analyses are performed in support of the investigation and reconstruction of actual fire incidents.

### 5.3 FIRE AND FLAMMABILITY TEST STANDARDS.

Regardless of the application, it is important that fire and flammability test methods be free of systematic error (bias). It is also essential that consistent results can be obtained from experiments repeated at different times within one laboratory (repeatability) and that there is reasonable agreement between the results for the same material, product, or assembly tested in different laboratories (reproducibility). Those are the reasons why fire safety codes, regulations, and specifications refer to standardized fire and flammability test methods and why test data needed in support of fire engineering are obtained with standardized experimental protocols.

#### 5.3.1 Consensus-Based Test Standards.

Most fire and flammability test standards are developed by consensus-based committees. The rules and procedures by which these committees operate ensure that the development cannot be dominated by a single interest group and that there is reasonable agreement between the different interest groups represented on the committee.

ASTM International (previously the American Society for Testing and Materials) and the National Fire Protection Association (NFPA) are the primary consensus-based organizations in the U.S. that develop and maintain fire and flammability test standards. Committee E05 on Fire Tests is the primary committee in ASTM that develops fire and flammability test standards [25]. Several material or product-oriented committees have subcommittees that develop fire and flammability test standards as well. For example, committee D20 on Plastics has a subcommittee on thermal properties (D20.30) that develops and maintains some fire and flammability test standards for plastics. The Fire Test Committee is responsible for all fire and flammability test standards that are used by any of the fire safety codes and standards published by NFPA. A number of test laboratories in the U.S., such as UL and FM Global, have established a consensus process that meets the requirements of the American National Standards Institute so that they now can publish American National Standards.



International fire and flammability test standards are developed by the International Organization for Standardization (ISO) and the International Electrotechnical Committee (IEC). The latter is concerned with electrical products only. Technical committees TC 92 and TC 89 are the primary committees that develop and maintain fire and flammability test standards in ISO and IEC respectively. As in ASTM, there are a number of product or industry-specific committees in ISO that also develop fire and flammability test standards. For example, SC1 on Test Methods of ISO TC 136 on Furniture has published two ignition tests for upholstered seating. An important difference between ISO and IEC versus ASTM and NFPA is that the international committees establish consensus on a geographical basis. Each country that actively participates in the work can be a voting member on an ISO or IEC committee. Committees are composed in a similar manner in CEN and CENELEC, which are the European counterparts of ISO and IEC respectively. However, member countries can have multiple votes in CEN and CENELEC committees. The number of votes is a function of the population of the country.

### 5.3.2 Other Types of Test Standards.

There are many fire and flammability tests methods that are not developed by a consensus-based process. In the U.S. these types of test standards are typically promulgated by regional or federal government agencies. The latter are published as part of the regulations that refer to these test methods in the Code of Federal Regulations (CFR), although many federal regulations rely on consensus-based test standards. Some federal fire and flammability test standards are also described in military specifications (MIL specs) issued by the different agencies of the Department of Defense. The U.S. government has recognized the advantages of using test standards that have been subjected to a review and are accepted by all interest groups and is now actively supporting the adoption of consensus-based tests standards. Examples of regional fire and flammability test standards that are not consensus-based are the California Technical Bulletins to assess the fire and flammability characteristics of upholstered furniture and mattresses. Finally, specifications for suppliers issued by manufacturers of passenger airplanes, railcars, etc., might also rely on fire and flammability test procedures that have not been developed by a consensus-based process. For example, Airbus, Boeing, and Bombardier all have their own fire and flammability test standards.

## 5.4 TESTING FOR REGULATORY COMPLIANCE.

There are literally hundreds of fire and flammability tests for polymers [5 and 25]; therefore, it is not possible to provide an overview of these tests in this report. A few important tests have been selected to illustrate the key concepts. These tests include the ones that are referred to in the first four sections of this report: the UL 94 20-mm Vertical Burning Test [27], the Limiting Oxygen Index Test [25], the Cone Calorimeter [25], and the Pyrolysis Combustion Flow Calorimeter [29]. For guidance on available fire and flammability test methods to evaluate polymers, the reader is referred to ASTM D 3814, “Standard Guide for Locating Combustion Test Methods for Polymeric Materials” [25]. A comprehensive review of fire and flammability tests used in support of codes and regulations in different parts of the world can be found in Troitzsch [5].

### 5.4.1 Typical Example of a Flammability Test.

The UL 94 standard provides procedures for bench-scale tests to determine the acceptability of plastic materials for use in appliances or other devices with respect to flammability under controlled laboratory conditions. The standard includes several test methods that are employed depending upon the intended end-use of the material and its orientation in the device. The standard outlines two horizontal burning tests, three vertical burning tests, and a radiant panel flame spread test. The most commonly used method is summarized below as a typical example of a flammability test.

The first vertical burning test described in the UL 94 standard is the 20-mm Vertical Burning Test; V-0, V-1, or V-2. The UL 94 test cabinet is shown in figure 23. The V-0, V-1, or V-2 classification is based on the duration of afterflaming or afterglowing following the removal of the burner flame, as well as the ignition of cotton by dripping particles from the test specimen.



Photo Courtesy of Fire Testing Technology ©2004

FIGURE 23. UL 94 CABINET

In this test, specimens measuring 125 mm in length by 13 mm wide are suspended vertically and clamped at the top end. A thin layer of cotton is positioned 300 mm below the test specimen to catch any molten material that may drop from the specimen. A 20-mm-long flame from a methane burner is applied to the center point on the bottom end of the specimen. The burner is positioned such that the burner barrel is located 10 mm below the bottom end of the material specimen. The flame is maintained for 10 seconds, and then removed to a distance of at least 150 mm. Upon flame removal, the specimen is observed for afterflaming and its duration time recorded ( $t_1$ ). As soon as the afterflame ceases, the burner flame is reapplied for an additional 10 seconds, then removed again. The duration of afterflaming ( $t_2$ ) or afterglowing ( $t_3$ ) are noted. Based on the results, the material is classified as either V-0, V-1, or V-2, based on the criteria outlined in table 8.

## 5.4.2 Typical Examples of Fire Tests.

The following two examples are commonly used tests that illustrate two distinct approaches to simulate the thermal exposure conditions in a preflashover compartment fire. The Steiner Tunnel Test uses a gas burner to heat the specimen, primarily by convection. The Radiant Flooring Panel test relies on a gas-fired panel that exposes a flooring specimen to a radiant heat flux profile.

### 5.4.2.1 The Steiner Tunnel Test.

The primary intent of the Steiner Tunnel Test is to quantify the wind-aided flame spread propensity of the material tested. It is the most common reaction-to-fire test method prescribed by U.S. model building codes. The Steiner Tunnel Test is described in ASTM E 84, “Standard Test Method for Surface Burning Characteristics of Building Materials,” and NFPA 255, “Standard Method of Test of Surface Burning Characteristics of Building Materials.” The apparatus, as shown in figure 24, consists of a long tunnel-like enclosure measuring 8.7 by 0.45 by 0.31 m. The test specimen is 7.6 m long and 0.51 m wide and is mounted in the ceiling position. It is exposed at one end, designated as the burner end, to a 79-kW gas burner. There is a forced draft through the tunnel from the burner end with an average initial air velocity of 1.2 m/s. A smoke photometer is mounted on the exhaust duct. The photometer consists of a white light source on one side of the duct and a photocell on the opposite side of the duct.



Photo Courtesy of Southwest Research Institute ©2004

FIGURE 24. THE STEINER TUNNEL TEST APPARATUS

The test measurements consist of flame spread over the surface and light absorption in the exhaust duct of the tunnel. The test duration is 10 minutes. A flame spread index (FSI) is calculated on the basis of the area under the curve of flame tip location versus time. The FSI is 0 for an inert board and is normalized to approximately 100 for red oak flooring. The smoke-developed index (SDI) is equal to 100 times the ratio of the area under the curve of light absorption versus time for the 10-minute test duration to the area under the curve for red oak flooring. Thus, the SDI of red oak flooring is 100, by definition.

The classification of linings in the model building codes in the U.S. is based on the FSI. There are three classifications: Class A, or I, for products with  $FSI \leq 25$ ; Class B, or II, for products with  $25 < FSI \leq 75$ ; and Class C, or III, for products with  $75 < FSI \leq 200$ . Class A, or I, products are generally permitted in stairways. Class B, or II, products can be used in corridors, and Class C, or III, products are allowed in other rooms and areas. The model building codes do not permit interior finishes that produce excessive amounts of light-obscuring smoke. Products that have to be tested according to the tunnel test must have an SDI of 450 or less.

#### 5.4.2.2 The Radiant Flooring Panel Test.

The National Bureau of Standards (NBS, currently the National Institute of Standards and Technology) conducted a series of full-scale fire tests in the 1970s to investigate the fire hazard of floor coverings. The main concern was flame spread from a fire room to a connected corridor. This work resulted in the development of the Radiant Flooring Panel Test. This test is described in ASTM E 648, “Standard Test Method for Critical Radiant Flux of Floor Covering Systems Using a Radiant Heat Energy Source” and NFPA 253, “Standard Method of Test for Critical Radiant Flux of Floor Covering Systems Using a Radiant Heat Energy Source.” The international version of this test method, ISO 9239-1 “Reaction to Fire Tests for Floor Coverings—Determination of the Burning Behavior Using a Radiant Heat Source,” includes a photometer in the exhaust stack to measure smoke optical density (see figure 25).



Photo Courtesy of Fire Testing Technology ©2004

FIGURE 25. THE RADIANT FLOORING PANEL TEST APPARATUS

The Radiant Flooring Panel Test apparatus consists of an air-gas-fueled radiant heat panel inclined at 30 degrees to and directed at a horizontally mounted floor covering system specimen. The radiant panel generates a heat flux distribution along the 1-m length of the test specimen

from a nominal maximum of  $10 \text{ kW/m}^2$  ( $1 \text{ W/cm}^2$ ) to a minimum of  $1 \text{ kW/m}^2$  ( $0.1 \text{ W/cm}^2$ ). The test is initiated by open-flame ignition from a pilot burner. The heat flux at the location of maximum flame propagation is reported as the critical radiant flux.

#### 5.4.2.3 Rate of Heat Release Test for Aircraft Cabin Materials.

The Federal Aviation Administration requires (14 CFR 25.853) that large areas, including interior ceiling and wall panels, partitions, galley structures, cabinets, and stowage compartments of commercial transport aircraft, pass a rate of heat release test in addition to flammability and smoke tests. The rate of heat release apparatus (see figure 26) is a modified version of the ASTM E-906, “Standard Test Method for Heat and Visible Smoke Release Rates of Materials and Products” (configuration A). Samples are 150- by 150-mm square and are cut from cabin components or tested in representative thickness. Samples are exposed to a radiant heat flux of  $35 \text{ kW/m}^2$  in a vertical orientation and ignited by an impinging pilot flame. The rate of heat released by flaming combustion is deduced from the calibrated temperature rise of the air stream passing over the sample surface at a prescribed flow rate. The maximum rate of heat release cannot be greater than  $65 \text{ kW/m}^2$  over the entire duration of the 5-minute test, and the heat released during the first 2 minutes of the test cannot be greater than  $65 \text{ kW-min/m}^2$ .

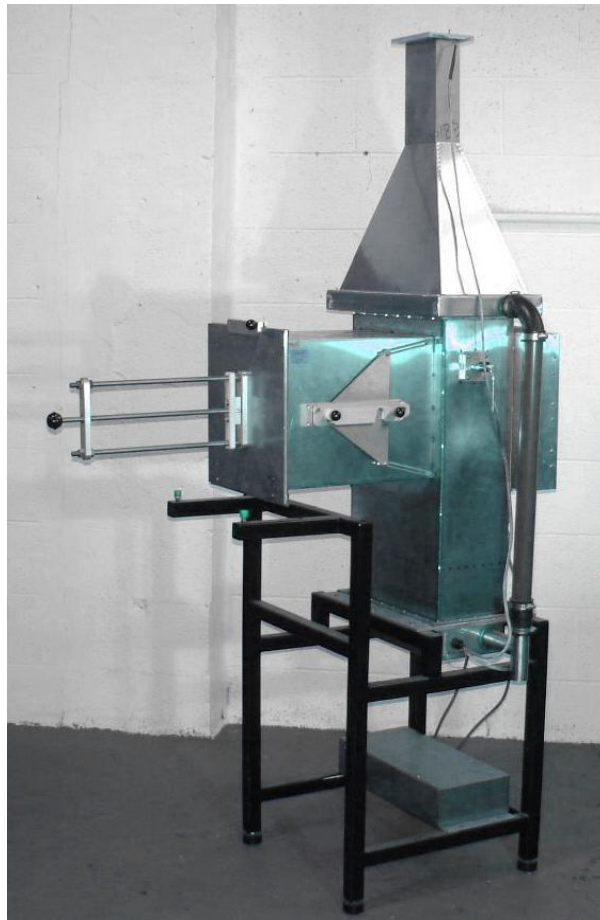


Photo Courtesy The Govmark Organization, Inc.

FIGURE 26. RATE OF HEAT RELEASE APPARATUS

## 5.5 TESTING FOR QUALITY ASSURANCE AND RESEARCH.

### 5.5.1 The LOI Test.

The LOI test is a typical example of a method that is used to control the production of materials, products, and assemblies and in research to develop new products. This test is standardized in North America as ASTM D 2863, “Standard Test Method for Measuring the Minimum Oxygen Concentration to Support the Candle-Like Combustion of Plastics (Oxygen Index),” and internationally as ISO 4589-2, “Plastics—Determination of Burning Behavior by Oxygen Index—Part 2: Ambient-Temperature Test.” The test does not correlate well with other fire and flammability tests nor does it provide a reliable indication of material performance in real fires. However, the results appear to be very sensitive to the composition of the material and the test is, therefore, ideally suited to serve as a quality assurance tool of fire-retardant-treated materials.

The LOI test apparatus consists of a glass tube 75 to 100 mm in diameter and 450 to 500 mm in height and is shown in figure 27. A specimen with a height between 70 and 200 mm and a width of 10 to 20 mm is supported inside the glass tube. A gas mixture of oxygen and nitrogen is supplied at the bottom of the tube and a small candle-like flame is applied to the top of the specimen in an attempt to ignite it. The objective is to find the minimum oxygen concentration in nitrogen that will result in sustained combustion for at least 3 minutes or excessive flame propagation down the specimen. The dimensions of the specimen and the limit of excessive flame propagation depend on the type of material that is being tested.



Photo Courtesy of Fire Testing Technology ©2004

FIGURE 27. THE LOI TEST APPARATUS

### 5.5.2 The Pyrolysis Combustion Flow Calorimeter.

The pyrolysis combustion flow calorimetry (PCFC) is a method for measuring quantitative flammability parameters of combustible materials and is used in research to develop new polymers with improved fire performance (Lyon and Walters 2004). In PCFC, the condensed-phase and gas-phase processes of flaming combustion are separately reproduced through controlled pyrolysis of milligram samples in an inert gas stream and high-temperature thermal oxidation (combustion) of the pyrolyzate in excess oxygen. The rate of heat released by combustion per unit mass of sample during the test (specific HRR, section 4.6) is measured by oxygen consumption calorimetry (section 4.2). Time-integration of the specific HRR gives the net heat of combustion of the fuel gases  $h_c^0$ . The maximum value of the specific HRR, normalized for the sample heating rate, is a material flammability parameter with the units and significance of a heat (release) capacity that is a good predictor of flame test results and fire performance. The temperature at maximum specific HRR is a good approximation of the ignition temperature (see sections 3.1, 4.4, and table A-1).

## 5.6 TESTING TO OBTAIN ENGINEERING DATA.

HRR is the primary characteristic to quantify the fire hazard of a material. Most fire tests to obtain engineering data, therefore, measure HRR. The rate of heat release is generally determined using oxygen consumption calorimetry. For a large number of organic liquids and gases [20], a nearly constant net amount of heat is released per unit mass of oxygen consumed for complete combustion. Sixty years later, researchers at NBS found this to also be true for organic solids and obtained an average value for this constant of 13.1 MJ/kg of O<sub>2</sub>. This value may be used for practical applications and is accurate with very few exceptions to within ±5%. Thornton's rule implies that it is sufficient to measure the oxygen consumed in a combustion system to determine the net heat released. This method, generally referred to as oxygen consumption calorimetry, is now the most widely used and accurate method for measuring HRR in experimental fires. A summary of the most commonly used oxygen consumption calorimeters follows.

### 5.6.1 Bench-Scale Calorimeters.

#### 5.6.1.1 The Cone Calorimeter.

The Cone Calorimeter is standardized in North America as ASTM E 1354, "Test Method for Heat and Visible Smoke Release Rates for Materials and Products Using an Oxygen Consumption Calorimeter," and internationally as ISO 5660-1, "Fire Tests – Reaction to Fire – Part 1: Rate of Heat Release From Building Products (Cone Calorimeter Method)." A commercial version of the Cone Calorimeter is shown in figure 28.

A 100- by 100-mm square sample is exposed to the radiant flux of an electric heater. The heater has the shape of a truncated cone (hence the name of the instrument) and is capable of providing heat fluxes to the specimen up to 100 kW/m<sup>2</sup>. An electric spark plug is used for the piloted ignition. The heater temperature is measured as an average of the readings from three thermocouples that are in contact with the coil. It is set and maintained at a certain level by a three-term controller. Calibration of heat flux as a function of heater temperature is performed

with a Schmidt-Boelter type total heat flux meter. Prior to testing, the heater temperature is set at the appropriate value, resulting in the desired heat flux.

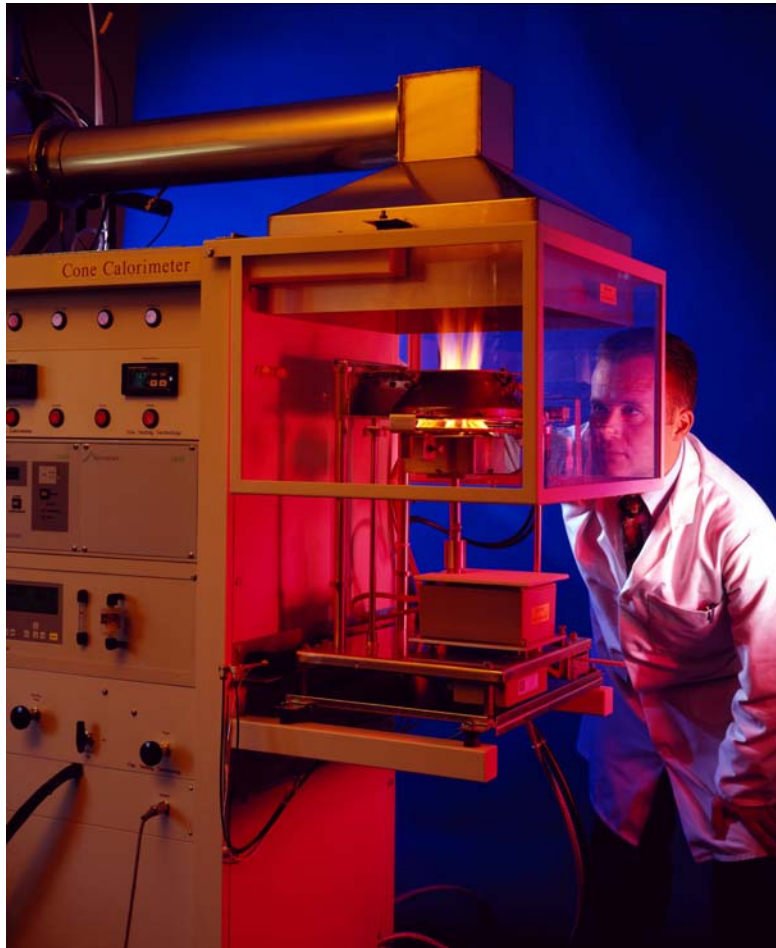


Photo Courtesy of Fire Testing Technology ©2004

FIGURE 28. COMMERCIAL VERSION OF THE CONE CALORIMETER

At the start of a test, the specimen in the appropriate holder is placed on the load cell, which is located below the heater. The load cell has a tare adjustment. This allows for a mechanical shift of the zero so that high accuracy mass loss measurements can be made, even if the mass of the holder and a possible substrate are much higher than the specimen. As soon as the pyrolysis products released by the specimen ignite, the electric spark plug is removed. All combustion products and entrained air are collected in the hood. An orifice plate at the entrance of the exhaust duct results in an almost uniform gas mixture. At a sufficient distance downstream from the mixing orifice, a gas sample is taken and analyzed for  $O_2$ . A laser photometer is located close to the gas-sampling point to measure light extinction by the smoke. The exhaust gases are removed by a high-temperature blower. The flow rate can be adjusted between 0 and 50 liters per second. For standard testing, the Cone Calorimeter is used in constant volume mode and the fan speed is set at 24 liters per second. Downstream of the fan is a second orifice plate. Measurements of the differential pressure across and gas temperature at the orifice plate are used for calculating the mass flow of the exhaust gases.



The Cone Calorimeter can also be used to obtain other data in support of fire safety engineering analysis. For example, the instrument can be used to determine ignition characteristics of a material by measuring the time to ignition at different heat flux levels. A laser smoke photometer is mounted on the duct to determine the smoke production rate. A continuous gas sample can be taken from the exhaust duct and analyzed to determine the concentration of different toxic and corrosive products of combustion in the effluents. Fourier Transform Infrared Spectroscopy is now a common method to measure the concentration of toxic and irritant gases in the exhaust duct of the Cone Calorimeter.

#### 5.6.1.2 The Fire Propagation Apparatus.

The Fire Propagation Apparatus was developed by FM Global Research (previously Factory Mutual Research Corporation). The test is described in ASTM E 2058, “Standard Test Methods for Measurement of Synthetic Polymer Material Flammability Using a Fire Propagation Apparatus (FPA).” A commercial version of the Fire Propagation Apparatus is shown in figure 29.

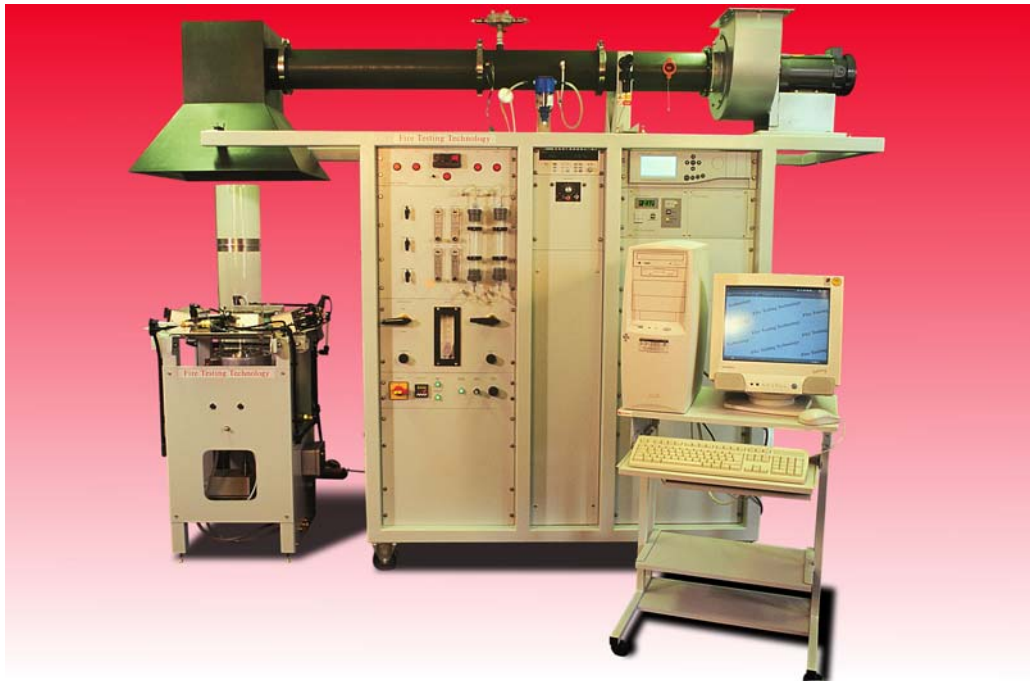


Photo Courtesy of Fire Testing Technology ©2004

FIGURE 29. COMMERCIAL VERSION OF THE FIRE PROPAGATION APPARATUS

The Fire Propagation Apparatus is similar to the Cone Calorimeter and can be used to obtain the same types of measurements. However, there are some significant differences that are briefly summarized below.

- The products of pyrolysis are ignited with a small hydrogen flame that is located 10 mm above the center of the specimen.

- The specimen is surrounded by a quartz tube. This makes it possible to conduct tests in a vitiated or oxygen-enriched atmosphere. The tube allows for a forced flow over the specimen surface and reduces the effect of external heat flux and specimen surface temperature on convective heat losses prior to ignition.
- Specimens are heated by high-temperature (approximately 2300 K) tungsten filament lamps that are located outside the quartz tube. Since the spectral response of many materials is different for a radiant heat source at this temperature compared to heat fluxes in fires from sources at much lower temperatures, specimens have to be blackened. In addition, due to the type of heaters that are used and the quartz tube arrangement, the maximum incident heat flux that can be obtained is 70 kW/m<sup>2</sup>.

## 5.6.2 Large-Scale Calorimeters.

### 5.6.2.1 The Room/Corner Test.

The Room/Corner Test is used to evaluate the fire growth characteristics of wall and ceiling linings. The walls and ceiling of a 2.4- by 3.6- by 2.4-m room are lined with the test material. A gas burner is placed in one of the rear corners of the room opposite the 0.8- by 2.0-m open doorway in the front wall. Products of combustion are collected in a hood located in front above the door opening and extracted by a high-temperature blower through the exhaust duct. The instrumentation in the exhaust duct is similar to that in the Cone Calorimeter, except the flow rate is typically determined on the basis of bidirectional probe measurements of centerline velocity and the smoke photometer often uses a white light source instead of a He-Ne laser. Several Room/Corner Test standards have been developed and are used for regulatory purposes. For example, NFPA 265, “Standard Methods of Fire Tests for Evaluating Room Fire Growth Contribution of Textile Wall Coverings,” is required in the U.S. to qualify textile wall coverings for use in unsprinklered spaces of certain types of buildings. ISO 9705, “Fire Tests – Full-Scale Room Test for Surface Products,” is more severe than NFPA 265 and is used to qualify materials as fire restricting for high-speed craft (small passenger ferries operating within a short distance from shore). Figure 30 shows an ISO 9705 test in progress.

### 5.6.2.2 The Furniture Calorimeter.

Often, it is very difficult to determine the burning behavior of complex objects on the basis of the fire performance of its individual components. For example, it is very hard to determine the burning behavior of upholstered furniture on the basis of the fire characteristics of the foam, fabric, and framing materials and to account for the geometry and configuration of the furniture and how it is ignited. It is much more practical to measure the HRR and related properties for the complete object. This can be done in a furniture calorimeter. The object is placed on a load platform to measure the mass loss rate during the test. It is ignited with a standardized ignition source and the products of combustion are collected in a hood and extracted through an exhaust duct. Measurements of oxygen concentration, flow rate, and light transmission in the exhaust duct are used to determine the HRR and smoke production rate from the object as a function of time. Furniture calorimeter test standards have been developed in ASTM for chairs, mattresses, and stacked chairs. The corresponding designations are ASTM E 1537, ASTM E 1590, and ASTM E 1822 respectively.



Photo Courtesy of Southwest Research Institute ©2004

FIGURE 30. ISO 9705 ROOM/CORNER TEST IN PROGRESS

### 5.6.2.3 The Intermediate-Scale Calorimeter.

One of the limitations of the Cone Calorimeter is that only relatively small samples can be evaluated. As a result, products that have joints or layered materials with a thickness exceeding 50 mm can generally not be tested in the Cone Calorimeter in a representative manner. For those types of products or assemblies, a larger calorimeter is required. Such an intermediate-scale calorimeter forms the subject of ASTM E 1623, “Standard Test Method for Determination of Fire and Thermal Parameters of Materials, Products, and Systems Using an Intermediate Scale Calorimeter (ICAL).”

The ICAL apparatus consists of an array of gas heaters, forming a vertical radiant panel with a height of approximately 1.33 m and width of approximately 1.54 m. The test specimen measures 1 by 1 m and is positioned parallel to the radiant panel. The heat flux to the specimen is preset to a maximum of  $60 \text{ kW/m}^2$  by adjusting the distance to the panel. Gas flow to the panel is controlled to maintain the temperature to the panel, and consequently, the heat flux to the specimen. The products of pyrolysis from the specimen are ignited with hot wires located close to, but not in contact with, the specimen at its top and bottom. The specimen is placed in a holder that is put on a load cell to measure mass loss during testing. The panel and specimen are positioned beneath the hood of the standard ISO 9705 room/corner test. All products of combustion are collected in the hood and continuously extracted through the exhaust duct. Instrumentation is provided in the duct for measuring HRR on the basis of oxygen consumption. A smoke photometer is also included for measuring smoke obscuration in the duct.

#### 5.6.2.4 The Fire Products Collector.

The first industrial-size calorimeter for fires into the megawatt (MW) range was built at Factory Mutual (currently FM Global) around 1980. This calorimeter, also referred to as the FM Fire Products Collector, was designed to measure heat and other fire products from test fires up to a size associated with sprinkler activation in commodity warehouse storage and other representative occupancies. Approximately 10 years later, a similar industrial-size calorimeter for HRR measurements up to 10 MW was constructed at SP National Testing Laboratory in Sweden. Since then several other laboratories, such as the National Research Council of Canada, the Fire Research Station in the UK, Underwriters Laboratories and Southwest Research Institute in the U.S. developed the capability of measuring HRR from large fires into the MW range.

#### 6. REFERENCES.

1. C.J. Hilado, *Flammability Handbook for Plastics*, 5<sup>th</sup> edition, Technomic Publishing Co., Lancaster, Pennsylvania, 1998.
2. A.H. Landrock, *Handbook of Plastics Flammability and Combustion Toxicology*, Noyes Publications, Park Ridge, NJ, 1983.
3. F.L. Fire, *Combustibility of Plastics*, Van Nostrand Reinhold, New York, 1991.
4. C.A. Harper, ed., *Handbook of Building Materials for Fire Protection*, McGraw-Hill, New York, NY, 2004.
5. Jürgen Troitzsch, *Plastics Flammability Handbook*, Hanser Publishers, Munich, 2004.
6. M.Le Bras, G. Camino, S. Bourbigot, and R. Delobel, *Fire Retardancy of Polymers: The Use of Intumescence*, The Royal Society of Chemistry, Cambridge, UK, 1998.
7. A.R. Horrocks and D. Price, eds., *Fire Retardant Materials*, Woodhead Publishing, Ltd., Cambridge, England, 2001.
8. G.L. Nelson, ed. *Fire and Polymers: Hazards Identification and Prevention*, ACS Symposium Series 425, American Chemical Society, Washington, D.C., 1990.
9. G.L. Nelson, ed., *Fire and Polymers II: Materials and Tests for Hazard Prevention*, ACS Symposium Series 599, American Chemical Society, Washington, D.C., 1995.
10. A.F Grand and C.A. Wilkie, eds., *Fire Retardancy of Polymeric Materials*, Marcel Dekker, Inc., NY, 2000.
11. The SFPE *Handbook of Fire Protection Engineering*, 3rd edition, Boston, MA, Society of Fire Protection Engineers, 2002.
12. D.D. Drysdale, *An Introduction to Fire Dynamics*, 2<sup>nd</sup> edition, John Wiley & Sons, New York, 1998.

13. G. Cox, ed., *Combustion Fundamentals of Fire*, Academic Press, Harcourt Brace & Co., Publishers, London UK, 1995.
14. R. Friedman, *Principles of Fire Protection Chemistry and Physics*, National Fire Protection Association, Quincy, MA, 1998.
15. C.F. Cullis and M.M. Hirschler, *The Combustion of Organic Polymers*, Clarendon Press, Oxford, England, 1981.
16. G. Pal and H. Macskasy, *Plastics: Their Behavior in Fires*, Elsevier, New York, 1991.
17. R.A. Strehlow, *Combustion Fundamentals*, McGraw-Hill, New York, 1984.
18. R. Turns, *An Introduction to Combustion— Concepts and Applications*, McGraw-Hill, New York, 1996.
19. I. Glassman, *Combustion*, 3rd ed., Academic Press, New York, 1996.
20. V. Babrauskas and S.J. Grayson, eds., *Heat Release in Fires*, Elsevier Applied Science, London, UK, 1992.
21. J.G. Quintiere, *Principles of Fire Behavior*, Del Mar Publishers, Albany, NY, 1998.
22. D.W. Van Krevelen, *Properties of Polymers*, 3rd ed., Elsevier Scientific, New York, 1990.
23. J.R. Hallman, "Ignition Characteristics of Plastics and Rubber," Ph.D. Thesis, the University of Oklahoma, 1971.
24. V. Babrauskas, *Ignition Handbook*, Fire Science Publishers, Issaquah, WA, 2003.
25. ASTM Fire Test Standards, Fifth Edition, American Society for Testing and Materials, West Conshohocken, PA, 1999.
26. R.E. Lyon and R.N. Walters, "Pyrolysis Combustion Flow Calorimetry," *Journal of Analytical and Applied Pyrolysis*, 71, 27-46 (2004)
27. Flammability of Plastic Materials, Northbrook, IL: Underwriters Laboratories Inc., UL 94 Section 2 (Horizontal: HB) and Section 3 (Vertical: V-0/1/2) 1991.
28. J. Bicerano, *Prediction of Polymer Properties*, 2<sup>nd</sup> edition, Marcel Dekker, Inc, NY, 1996.
29. R.N. Walters and R.E. Lyon, "Molar Group Contributions to Polymer Flammability," *Journal of Applied Polymer Science*, 87, 548-563, 2003.

APPENDIX A—TABULAR DATA FOR POLYMERS

TABLE A-1. ONSET DECOMPOSITION ( $T_d$ ), PEAK MASS LOSS RATE ( $T_p$ ), AND IGNITION ( $T_{ign}$ ) TEMPERATURES OF POLYMERS (AVERAGE VALUES  $\pm 10^\circ\text{C}$ )

POLYMER	ISO/ASTM Abbreviation	$T_d$ °C	$T_p$ °C	$T_{ign}$ °C
Thermoplastics				
Acrylonitrile-butadiene-styrene	ABS	390	461	394
ABS FR	ABS-FR	–	–	420
Polybutadiene	BDR	388	401	378
Polyisobutylene (butyl rubber)	BR	340	395	330
Cellulose Acetate	CA	250	310	348
Cyanate Ester (typical)	CE	448	468	468
Polyethylene (chlorinated)	CPE	448	476	–
Polyvinylchloride (chlorinated)	CPVC	–	–	643
Polychloroprene rubber	CR	345	375	406
Polychlorotrifluoroethylene	CTFE	364	405	580
Poly(ethylene-chlorotrifluoroethylene)	ECTFE	445	465	613
Phenoxy-A	EP	–	350	444
Epoxy (EP)	EP	427	462	427
Poly(ethylene-tetrafluoroethylene)	ETFE	490	520	540
Polyethylenevinylacetate	EVA	448	473	
Fluorinated ethylene propylene	FEP	–	–	630
Poly(styrene-butadiene)	HIPS	327	430	413
Poly(styrene-butadiene) FR	HIPS-FR	–	–	380
Poly(p-phenyleneterephthalamide)	KEVLAR	474	527	–
Polyarylate (liquid crystalline)	LCP	514	529	–
Melamine formaldehyde	MF	350	375	350
Polyisoprene (natural rubber)	NR	301	352	297
Polytrifluoroethylene	P3FE	400	405	–
Polyamide 12	PA12	448	473	–
Polyamide 6	PA6	424	454	432
Polyamide 610	PA610	440	460	–
Polyamide 612	PA612	444	468	–
Polyamide 66	PA66	411	448	456
Polyamide 6 (glass reinforced)	PA6-G	434	472	390
Polyamideimide	PAI	485	605	526
Polyacrylamide	PAM	369	390	–
Polyacrylonitrile	PAN	293	296	460
Polyarylate (amorphous)	PAR	469	487	–

TABLE A-1. ONSET DECOMPOSITION ( $T_d$ ), PEAK MASS LOSS RATE ( $T_p$ ), AND IGNITION ( $T_{ign}$ ) TEMPERATURES OF POLYMERS (AVERAGE VALUES  $\pm 10^\circ\text{C}$ ) (Continued)

POLYMER	ISO/ASTM Abbreviation	$T_d$	$T_p$	$T_{ign}$
		$^\circ\text{C}$	$^\circ\text{C}$	$^\circ\text{C}$
Thermoplastics				
Polybutene	PB	–	390	–
Polybenzimidazole	PBI	584	618	–
Polybutylmethacrylate	PBMA	261	292	–
Polybenzobisoxazole	PBO	742	789	–
Polybutyleneterephthlate	PBT	382	407	382
Polybutyleneterephthalate	PBT-G	386	415	360
Polycarbonate	PC	476	550	500
Polycarbonate/ABS (70/30)	PC/ABS	421	475	440
Polycarbonate (glass reinforced)	PC-G	478	502	420
Polycaprolactone	PCL	392	411	–
Polyethylene (high density)	PE HD	411	469	380
Polyethylene (low density)	PE LD	399	453	377
Polyethylacrylate	PEA	373	404	–
Polyethylene-acrylic acid salt	PEAA	452	474	–
Polyetheretherketone	PEEK	570	600	570
Polyetherimide	PEI	527	555	528
Polyetherketone (e.g., KADEL)	PEK	528	590	–
Polyetherketoneketone	PEKK	569	596	–
Polyethylmethacrylate	PEMA	246	362	–
Polyethylenenaphthalate	PEN	455	495	479
Polyethyleneoxide	PEO	373	386	–
Polyethersulfone	PESU	533	572	502
Polyethyleneterephthlate	PET	392	426	407
Phenol formaldehyde	PF	256	329	429
Polytetrafluoroethylene-perfluoroether	PFA	–	578	–
Phenol formaldehyde	PF-G	–	–	580
Polymethylmethacrylate	PMMA	354	383	317
Poly(4-methyl-1-pentene)	PMP	–	377	–
Poly( $\alpha$ -methyl)styrene	PMS	298	333	–
Poly( $\alpha$ -methylstyrene)	PMS	250	314	–
Polyoxymethylene	POM	323	361	344
Polypropylene	PP	354	424	367
Polypropylene (isotactic)	PP (iso)	434	458	–

TABLE A-1. ONSET DECOMPOSITION ( $T_d$ ), PEAK MASS LOSS RATE ( $T_p$ ), AND IGNITION ( $T_{ign}$ ) TEMPERATURES OF POLYMERS (AVERAGE VALUES  $\pm 10^\circ\text{C}$ ) (Continued)

POLYMER	ISO/ASTM Abbreviation	$T_d$ °C	$T_p$ °C	$T_{ign}$ °C
Thermoplastics				
Polyphthalamide (AMODEL)	PPA	447	488	–
Polyphenyleneether	PPE	–	418	426
Poly(2,6-dimethylphenyleneoxide)	PPO	441	450	418
Polypropyleneoxide	PPOX	292	343	–
Polyphenylenesulfide	PPS	504	545	575
Polyphenylsulfone	PPSU	557	590	575
Polystyrene	PS	319	421	356
Polysulfone	PSU	481	545	510
Polytetrafluoroethylene	PTFE	545	590	630
Polytetramethyleneoxide	PTMO	–	352	–
PU (isocyanurate/rigid)	PU	271	422	378
Polyetherurethane rubber	PUR	324	417	356
Polyvinylacetate	PVAC	319	340	–
Polyvinylbutyral*	PVB	333	373	–
Polyvinylchloride (50% DOP)	PVC (flex)	249	307	318
Polyvinylchloride (rigid)	PVC (rigid)	273	285	395
Polyvinylchloride/polyvinylacetate blend	PVC/PVAC	255	275	–
Polyvinylidenechloride	PVDC	225	280	–
Polyvinylidene fluoride	PVDF	440	490	643
Polyvinyl fluoride	PVF	361	435	476
Polyvinylcarbazole	PVK	356	426	–
Polyvinylalcohol	PVOH	298	322	–
Polyvinylpyridine	PVP	385	408	–
Polypara(benzoyl)phenylene	PX	476	602	–
Poly(styrene-acrylonitrile)	SAN	389	412	368
Phenylsilsesquioxane (silicone) Resin	SI	475	541	–
Silicone Rubber	SIR	456	644	407
Poly( styrene-maleic anhydride)	SMA	337	388	–
Polyimide thermoplastic	TPI	523	585	600
Polyurethane thermoplastic	TPU	314	337	271
Unsaturated Polyester	UPT	330	375	380
Unsaturated Polyester	UPT-G	–	–	395



TABLE A-2. LATENT HEAT OF GASIFICATION, CHAR YIELD, AND ENTHALPY OF GASIFICATION OF POLYMERS

Polymer	$L_g$	$\mu$	$h_g$
	kJ/g	g/g	kJ/g
ABS	2.3	0.00	2.3
ABS-FR	2.5	0.00	2.5
CEA	4.0	0.36	2.6
CEE	4.1	0.42	2.4
CEF	3.0	0.55	1.3
CEM	3.0	0.26	2.2
CEN	3.0	0.52	1.4
CET	3.5	0.35	2.3
CPE (25% CI)	2.1	0.00	2.1
CPE (36% CI)	2.8	0.20	2.2
CPVC	2.0	0.00	2.0
CR	2.0	0.13	1.7
ECTFE	1.5	0.00	1.5
EP	1.6	0.04	1.5
EPDM	1.9	0.00	1.9
EP (30% fiberglass)	2.3	0.30	1.6
ETFE	1.1	0.00	1.1
FEP	1.5	0.00	1.5
HIPS	2.0	0.00	2.0
HIPS-FR	2.1	0.10	1.9
PA6	1.5	0.02	1.5
PA66	2.1	0.04	2.0
PAI	4.8	0.61	1.9
PBI	5.5	0.75	1.4
PBT	1.4	0.07	1.3
PBT-FR	2.3	0.15	2.0
PC	2.4	0.25	1.8
PC-FR	3.5	0.52	1.7
PE HD	2.2	0.00	2.2
PE LD	1.9	0.00	1.9
PEEK	3.4	0.54	1.6
PEI	3.5	0.53	1.7
PEN	2.5	0.18	2.0
PESU	3.8	0.40	2.3
PET	1.4	0.05	1.3
PF	5.4	0.60	2.2

TABLE A-2. LATENT HEAT OF GASIFICATION, CHAR YIELD, AND ENTHALPY OF GASIFICATION OF POLYMERS (Continued)

Polymer	$L_g$	$\mu$	$h_g$
	kJ/g	g/g	kJ/g
PMMA	1.7	0.00	1.7
POM	2.4	0.00	2.4
PP	1.9	0.00	1.9
PPS	3.8	0.50	1.9
PPSU	4.3	0.58	1.8
PS	1.8	0.00	1.8
PSU	2.0	0.28	1.4
PTFE	2.5	0.00	2.5
PU	2.3	0.13	2.0
PVC (flexible)	1.3	0.08	1.2
PVC (rigid)	2.3	0.09	2.1
PVDF	4.0	0.23	3.1
PVF	1.9	0.00	1.9
PX	6.4	0.66	2.2
SIR	2.3	0.00	2.3
TPU	2.4	0.13	2.1

TABLE A-3. POLYMER THERMAL CONDUCTIVITY, DENSITY, HEAT CAPACITY, AND THERMAL DIFFUSIVITY AT ROOM TEMPERATURE

Polymer	$\kappa$ (W/m-K)	$\rho$ (kg/m <sup>3</sup> )	$c_p$ (kJ/kg-K)	$\alpha$ (m <sup>2</sup> /s x 10 <sup>7</sup> )
ABS	0.26	1050	1.50	1.65
BDR	0.22	970	1.96	1.16
BR	0.13	920	1.96	0.72
CA	0.25	1250	1.67	1.20
CAB	0.25	1200	1.46	1.43
CAP	0.25	1205	1.46	1.42
CE	0.19	1230	1.11	1.39
CN	0.23	1375	1.46	1.15
CP	0.20	1300	1.46	1.05
CPVC	0.48	1540	0.78	4.00
CR	0.19	1418	1.12	1.20
CTFE	0.23	1670	0.92	1.50
DAP	0.21	1350	1.32	1.18
DAP-G	0.42	1800	1.69	1.38

TABLE A-3. POLYMER THERMAL CONDUCTIVITY, DENSITY, HEAT CAPACITY, AND THERMAL DIFFUSIVITY AT ROOM TEMPERATURE (Continued)

Polymer	$\kappa$ (W/m-K)	$\rho$ (kg/m <sup>3</sup> )	$c_p$ (kJ/kg-K)	$\alpha$ (m <sup>2</sup> /s x 10 <sup>7</sup> )
EAA	0.26	945	1.62	1.70
ECTFE	0.16	1690	1.17	0.81
EP	0.19	1200	1.7	1.12
EPDM	0.20	930	2.0	1.08
EP-G	0.42	1800	1.60	1.46
EPN	0.19	1210	1.26	1.25
ETFE	0.24	1700	1.0	0.66
EVA	0.34	930	1.37	2.67
FEP	0.25	2150	1.17	0.99
HIPS	0.22	1045	1.4	1.54
LCP	0.20	1350	1.20	1.24
MF	0.25	1250	1.67	1.20
MF-G	0.44	1750	1.67	1.51
NBR	0.25	1345	1.33	1.40
NR	0.14	920	1.55	0.98
P3FE	0.31	1830	1.08	1.41
PA11	0.28	1120	1.74	1.44
PA11-G	0.37	1350	1.76	1.56
PA12	0.25	1010	1.69	1.46
PA6	0.24	1130	1.55	1.37
PA610	0.23	1100	1.51	1.38
PA612	0.22	1080	1.59	1.28
PA66	0.23	1140	1.57	1.29
PA6-G	0.22	1380	1.34	1.19
PAEK	0.30	1300	1.02	2.27
PAI	0.24	1420	1.00	1.69
PAN	0.26	1150	1.30	1.74
PAR	0.18	1210	1.20	1.24
PB	0.22	920	2.09	1.14
PBI	0.41	1300	0.93	3.40
PBT	0.22	1350	1.61	1.01
PC	0.20	1200	1.22	1.36
PC-G	0.21	1430	1.10	1.34
PE (HD)	0.43	959	2.00	2.24
PE (LD)	0.38	925	1.55	2.65
PE (MD)	0.40	929	1.70	2.53



TABLE A-3. POLYMER THERMAL CONDUCTIVITY, DENSITY, HEAT CAPACITY, AND THERMAL DIFFUSIVITY AT ROOM TEMPERATURE (Continued)

Polymer	$\kappa$ (W/m-K)	$\rho$ (kg/m <sup>3</sup> )	$c_p$ (kJ/kg-K)	$\alpha$ (m <sup>2</sup> /s x 10 <sup>7</sup> )
PVK	0.16	1265	1.23	1.02
PVOH	0.20	1350	1.55	0.96
PX	0.32	1220	1.3	2.02
SAN	0.15	1070	1.38	1.02
SBR	0.17	1100	1.88	0.82
SI-G	0.30	1900	1.17	1.35
SIR	0.23	970	1.59	1.49
UF	0.25	1250	1.55	1.29
UPT	0.17	1230	1.30	1.06
UPT-G	0.42	1650	1.05	1.85
VE	0.25	1105	1.30	1.74

TABLE A-4. SURFACE ABSORPTIVITY OF POLYMERS

Polymer	Radiant Energy Source			
	1000 K Blackbody	1500 K Blackbody	Flames	Solar
BR	0.92	0.93	0.92	0.95
CR	0.72	0.63	0.71	0.62
HIPS	0.86	0.75	0.88	0.29
NR	0.88	0.82	0.89	0.69
PA66	0.93	0.90	0.93	0.63
PC	0.87	0.83	0.88	0.69
PE LD	0.92	0.88	0.93	0.57
PMMA (black)	0.94	0.94	0.94	0.96
PMMA (clear)	0.85	0.69	0.89	0.097
PP	0.87	0.83	0.86	0.62
PPO	0.86	0.78	0.88	0.48
PS (clear)	0.75	0.60	0.78	0.095
PVC (flex)	0.90	0.90	0.91	0.89
SIR	0.79	0.66	0.79	0.62

TABLE A-5. EFFECTIVE HEAT OF COMBUSTION, HEAT OF COMPLETE COMBUSTION OF FUEL GASES ( $h_c^0$ ), AND FLAMING COMBUSTION EFFICIENCY ( $\chi$ )

Polymer	HOC (kJ/g)	$h_c^0$ (kJ/g)	$\chi$
CEN	20.6	20.7	1.00
CEE	25.1	25.3	0.99
PMMA	24.8	25.0	0.99
PP	41.9	43.0	0.97
PE LD	40.3	41.4	0.97
PUR	24.0	24.7	0.97
PE HD	40.3	41.6	0.97
CET	25.9	26.9	0.96
PAI	15.3	15.9	0.96
CR	17.6	18.5	0.95
CEM	28.9	30.6	0.94
PEI	21.8	23.2	0.94
CEA	25.9	27.6	0.94
UPT	23.4	25.0	0.94
POM	14.4	15.4	0.94
TPU	23.5	25.4	0.93
PPA	24.2	26.2	0.92
CEF	16.9	18.3	0.92
PA66	25.2	27.4	0.92
PEEK	21.3	23.2	0.92
PBT	21.7	23.8	0.91
PSU	20.4	22.4	0.91
PC	21.2	23.3	0.91
PEN	22.9	25.2	0.91
PPZ	15.0	16.6	0.90
PESU	22.4	24.9	0.90
PA6	25.8	28.7	0.90
PPSU	23.5	27.0	0.87
PPS	25.4	29.3	0.87
PBI	22.0	26.5	0.83
SBR	31.5	38.0	0.83
EVA	30.8	37.9	0.81
NR	30.2	37.9	0.80
SIR	21.7	27.2	0.80
PPO/PS	21.3	26.9	0.79
ABS	29.0	36.6	0.79

TABLE A-5. EFFECTIVE HEAT OF COMBUSTION, HEAT OF COMPLETE COMBUSTION OF FUEL GASES ( $h_c^0$ ), AND FLAMING COMBUSTION EFFICIENCY ( $\chi$ ) (Continued)

Polymer	HOC (kJ/g)	$h_c^0$ (kJ/g)	$\chi$
EPDM	29.2	37.9	0.77
CTFE	6.5	8.5	0.76
HIPS	28.1	37.2	0.76
EP	20.4	27.1	0.75
PET	18.0	24.1	0.75
LCP	14.8	20.6	0.72
CPE (25% Cl)	22.6	31.6	0.72
VE	22.0	31.1	0.71
ETFE	7.3	10.8	0.68
PS	27.9	42.0	0.66
PU	16.3	25.4	0.64
PX	20.0	31.3	0.64
PVC (flexible)	11.3	19.3	0.59
PTFE	4.6	8.4	0.55
PVC (rigid)	9.3	18.6	0.50
PS-FR	13.8	33.0	0.42
CPE (36% Cl)	10.6	26.3	0.40
TPI	12.0	31.6	0.38
ABS-FR	10.2	26.9	0.38
PVDF	3.8	10.4	0.36
CPE (48% Cl)	7.2	20.2	0.36
ECTFE	4.6	13.6	0.34
CPVC	3.9	12.8	0.30
PVF	4.1	18.5	0.22
FEP	1.3	7.7	0.17

TABLE A-6. LIMITING HEAT RELEASE RATE ( $HRR_0$ ), HEAT RELEASE PARAMETER, LIMITING OXYGEN INDEX, UL 94 RATING, AND HEAT RELEASE CAPACITY ( $\eta_c$ )

Polymer	$HRR_0$ (kW/m <sup>2</sup> )	HRP (kJ/kJ)	LOI, [O <sub>2</sub> ] (% v/v)	UL 94 Rating	$\eta_c$ (J/g-K)
HIPS	510 ±77	14 ±2	18	HB	893
PP	369 ±79	22 ±2	17	HB	1200
PET	424 ±168	13 ±4	20	HB	402
PS	410 ±66	17 ±2	18	HB	1040
ABS	359 ±66	13 ±2	18	HB	669
PBT	341 ±106	15 ±3	23	HB	474
PE (chlorinated)	–	–	21	HB	693
UPT	261 ±105	11 ±2	20	HB	–
PC/ABS	259 ±43	11 ±1	–	HB	–
PA66	240 ±59	18 ±2	24	HB	600
PMMA	217 ±47	13 ±1	17	HB	574
PS-FR	205 ±27	7 ±1	–	V2	–
PPO/PS	192 ±22	15 ±1	–	HB	–
PA6	187 ±55	18 ±2	24	HB	487
PC/ABS-FR	178 ±36	7 ±1	–	V1	–
VET	169 ±44	13 ±1	–	HB	805
PESU	168 ±23	4 ±0	36	V1	345
HIPS-FR	164 ±30	5 ±1	–	V2	–
POM	162 ±30	6 ±1	15	HB	398
EP	160 ±46	10 ±1	19	HB	657
PE	145 ±93	21 ±3	17	HB	1560
PBT-FR	141 ±130	6 ±3	–	V2	–
CEA	112 ±22	7 ±2	24	V1	273
ABS-FR	117 ±33	6 ±1	–	V2	301
HIPS-FR	114 ±36	4 ±1	–	V0	–
PVC (flex)	91 ±19	4 ±0	–	V2	–
SIR (filled)	90 ±13	5 ±0	32	V0	88
PC	89 ±32	9 ±1	25	V2	390
PEN	57 ±13	5 ±0	32	V2	309
ETFE	44 ±31	6 ±0	30	V0	198
PVC (rigid)	9 ±25	3 ±1	45	V0	138
CR	–	9	40	V0	188
KEVLAR	–	–	32	V0	302

HB = Horizontal burning  
V = vertical



TABLE A-6. LIMITING HEAT RELEASE RATE ( $HRR_0$ ), HEAT RELEASE PARAMETER, LIMITING OXYGEN INDEX, UL 94 RATING, AND HEAT RELEASE CAPACITY ( $\eta_c$ ) (Continued)

Polymer	$HRR_0$ (kW/m <sup>2</sup> )	HRP (kJ/kJ)	LOI, [O <sub>2</sub> ] (% v/v)	UL 94 Rating	$\eta_c$ (J/g-K)
UPT-FR	-31 ±10	2 ±0	–	V0	–
CPVC	-34 ±9	3 ±0	52	V0	–
PE (crosslinked)-FR	-38 ±28	5 ±5	–	V0	–
PAI	-64 ±16	2 ±0	45	V0	33
PPSU	-83 ±25	4 ±0	38	V0	115
PTFE	-84 ±9	2 ±0	95	V0	35
PEEK	-94 ±20	3 ±0	35	V0	155
NOMEX	–	–	28	V0	152
PEI	-113 ±19	3 ±0	47	V0	121
ECTFE	-127 ±6	4 ±0	60	V0	–
PPS	-147 ±30	6 ±1	44	V0	164
PBI	-150 ±36	3 ±0	36	V0	41
PC-FR	-191 ±51	4 ±1	56	V0	30
FEP	–	2	95	V0	57

HB = Horizontal burning  
V = vertical

TABLE A-7. SMOKE EXTINCTION AREA OF POLYMERS

Polymer	Smoke Extinction Area (m <sup>2</sup> /kg)
PTFE	33
CPVC	33
POM	50
Douglas Fir (wood)	75
PI	75
PMMA	100
PBI	100
PAI	120
PA6	134
Hemlock (wood)	150
PEI	150
PES	150

TABLE A-7. SMOKE EXTINCTION AREA OF POLYMERS (Continued)

Polymer	Smoke Extinction Area (m <sup>2</sup> /kg)
PA66	230
PEEK	292
PAS	300
PE	325
PF	325
PET	400
PP	455
PSU	475
PU	550
PBT	623
PPS	646
PVC flex/FR	770
PEKK	800
UPT	800
PC	891
PMMA/PVC alloy	900
EP	907
ABS	925
BMI	950
PVC rigid	1015
VE	1050
PVC flex	1078
PS	1150
PPO	1300
ABS (Br FR)	1500
Silicone Elastomers	1500
EP (Br FR)	1600
PS (Br FR)	1650